T.C.

TOKAT GAZİOSMANPAŞA UNIVERSITY

GRADUATE EDUCATION INSTITUTE

DEPARTMENT OF MECHATRONIC ENGINEERING

DEVELOPMENT OF A NEW ONLINE MEASUREMENT SYSTEM TO MONITOR THE AIR QUALITY OF ANIMAL HOUSING

MASTER'S THESIS

Djoro Sem Samuel GNEPA

Advisor : Prof. Dr. Sefa TARHAN

TOKAT –2025

THESIS STATEMENT

Scientific ethics were used in the writing of this thesis, which was prepared in accordance with the thesis writing rules. scientific rules are respected, and in the event of benefit from the work of others, scientists that it is cited in accordance with the standards, that the innovations and results contained in the thesis are that they have not been taken from somewhere, that the data used have not been falsified and that the thesis any part originating from another thesis work in this or another university. I declare that it is not presented as such.

………./………/2025

Djoro Sem Samuel GNEPA

ÖZET

HAYVAN BARINAĞINDA HAVA KALİTESİNİ İZLEMEK İÇİN YENİ BİR ÇEVRİMİÇİ ÖLÇÜM SİSTEMİNİN GELİŞTİRİLMESİ

Djoro Sem Samuel, GNEPA
Yüksek Lisans, Mekatronik Mühendisliği Anabilim Dalı
Tez Danışmanı: Prof.Dr. Sefa TARHAN
Ocak 2025, xiv + 78 sayfa

Hayvan barınaklarında optimal hava kalitesinin korunması, çiftlik hayvanlarının sağlığı, refahı ve verimliliği açısından büyük önem taşımaktadır. Kötü hava kalitesi, hayvanları amonyak (NH_3), metan (CH_4) ve karbondioksit (CO_2) gibi zararlı gazlara maruz bırakarak solunum hastalıklarına, strese ve düşük verimliliğe neden olabilmektedir. Ayrıca, bu emisyonlar sera gazı birikimi ve iklim değişikliği gibi çevresel sorunlara da neden olabilmektedirler. Bu nedenle, hava kalitesi parametrelerinin sürekli izlenmesi ve değerlendirilmesi, etkili bir hayvancılık yönetimi için gereklidir. Bu çalışmanın amacı, ahırlarda kullanmak için mevcut sensörleri kullanarak gerçek zamanlı bir hava kalitesi izleme sistemi geliştirmektir. Sistem, bir PCB üzerinde çeşitli gaz sensörlerini ve bir sıcaklık-nem sensörünü entegre eden Arduino Nano mikrodenetleyici tarafından yönetilmektedir. Kullanılan sensörler arasında TGS2611-E00 metan sensörü, SHT35 nem ve sıcaklık sensörü, MH-Z16 NDIR karbondioksit sensörü, KE-25 oksijen sensörü ve MQ137 amonyak sensörü bulunmaktadır. Metan ve Amonyak sensörlerinin düşük gaz konstrasyonlarını doğru ölçebilmeleri için literatürde verilen kalibrasyon eşitlikleri kullanılmıştır. Diğer sensörlerin üretici firmalar tarafından kalibre edildiği için ayrı bir kalibrasyona ihtiyaç duyulmamaştır. Sensörlerden gelen çıkış sinyalleri analogdan dijitale çevirici (ADC) aracılığıyla işlenmekte ve LoRa iletişim protokolü kullanılarak kablosuz olarak merkezi bir iklim birimine iletilmektedir. Bu çalışmanın önemli bir yönü, sensörlerden elde edilen verilerin analiz edilerek ahır içindeki hava kalitesinin değerlendirilmesi ve izlenmesidir. Elde edilen sonuçlar kritik eşik değerleriyle karşılaştırılarak hayvan refahı üzerindeki etkileri incelenmiştir. Ahır içi sıcaklık ve bağıl nem değerleri

kullanılarak sıcaklık ve bağıl nem indeks değerleri hesaplanmıştır. Bu indeks ısıl stresin takip edilmesinde kullanılabilir. Ayrıca, hava kalitesindeki olumsuz değişimlerin şiddetini ve süresini belirlemek için günlük stres yükü değeri ve günlük stres süresi olarak iki farklı değer belirlenmiştir. Gerçek zamanlı hava kalitesi değerlendirmesini entegre eden bu sistem, çiftçilerin havalandırmayı optimize etmelerine, zararlı gaz birikimini azaltmalarına ve ahır koşullarını iyileştirmelerine yardımcı olacak önemli bir araç sunmaktadır.

Anahtar Kelimeler: Dijital Hayvancılık, Hava Kalitesi, Hayvan Konforu, Çevresel Veri, Hayvan stresi

ABSTRACT

DEVELOPMENT OF A NEW ONLINE MEASUREMENT SYSTEM TO MONITOR THE AIR QUALITY OF ANIMAL HOUSING

Djoro Sem Samuel, GNEPA

Master's Thesis, Department of Mechatronic Engineering

Advisor: Prof.Dr. Sefa TARHAN

January 2025, xiv + 78 pages

Maintaining optimal air quality in animal barns is of great importance for the health, welfare and productivity of farm animals. Poor air quality can expose animals to harmful gases such as ammonia (NH_3), methane (CH_4) and carbon dioxide (CO_2), which can cause respiratory diseases, stress and low productivity. In addition, these emissions can cause environmental problems such as greenhouse gas accumulation and climate change. Therefore, continuous monitoring and evaluation of air quality parameters are necessary for effective livestock management. The aim of this study is to develop a real-time air quality monitoring system using existing sensors for use in barns. The system is managed by an Arduino Nano microcontroller that integrates various gas sensors and a temperature-humidity sensor on a PCB. The sensors used include TGS2611-E00 methane sensor, SHT35 humidity and temperature sensor, MH-Z16 NDIR carbon dioxide sensor, KE-25 oxygen sensor and MQ137 ammonia sensor. In order for Methane and Ammonia sensors to measure low gas concentrations accurately, the calibration equations given in the literature were used. Since other sensors were calibrated by the manufacturers, no separate calibration was required. The output signals from the sensors are processed via an analog-to-digital converter (ADC) and transmitted wirelessly to a central climate unit using the LoRa communication protocol. An important aspect of this study is the evaluation and monitoring of air quality inside the barn by analyzing the data obtained from the sensors. The results obtained were compared with critical threshold values and their effects on animal welfare were examined. Temperature

and relative humidity index values were calculated using barn temperature and relative humidity values. This index can be used to monitor thermal stress. In addition, two different values were determined as daily stress load value and daily stress duration to determine the severity and duration of negative changes in air quality. This system, which integrates real-time air quality assessment, provides an important tool that will help farmers optimize ventilation, reduce harmful gas accumulation and improve barn conditions.

Keywords: Digital Livestock Farming, Calibration Greenhouse Gases, Air Quality, Animal Comfort, Environmental data, Animal stress

ACKNOWLEDGEMENTS

I wish to extend my heartfelt gratitude to my supervisor, Prof. Dr. Sefa TARHAN, for his unwavering support, guidance, and encouragement, which have greatly enriched my learning experience during my graduate studies. I am equally thankful to all the professors involved in the master's program for their professional guidance in the development and completion of this thesis.

This work would not have been possible without the support and motivation provided by my classmates and family. I am deeply appreciative of the financial support given by TÜBITAK (Project Number : 223N226) . My sincere thanks go to Assist. Prof. Dr. Kenan Zengin for his invaluable contributions.

I am also grateful to my fellow Ivorians in Türkiye, as well as the staff and faculty members of the School of Mechatronic Engineering at Tokat Gaziosmanpasa University, for their collaboration over the past two years.

A special thanks goes to my parents for their constant encouragement and unwavering belief in my ability to achieve my goals. Lastly, I express my heartfelt appreciation to all those who contributed to the completion of this thesis, even if their names are not mentioned here. You all made my time living and studying in Tokat a truly memorable and rewarding experience.

CONTENTS

LISTES OF TABLES

LIST OF FIGURES

SYMBOLS and ABBREVIATIONS

SYMBOLS	DESCRIPTION
ADC	Analog to Digital converter
ASTM	Standard Test Method for Measuring Humidity with a Psychrometer
CSS	Chirp Spread Spectrum (CSS)
DHT	Temperature and Humidity sensor
DSD	Daily Stress Duration
DSLV	Daily Stress Load Value
Eq	Equivalent
GHG	Greenhouses Gas
GND	Ground
IDE	Integrated Development Environment
ISD	Individual Stress Duration
ISLV	Individual Stress Load Value
LoRa	Long Range
MV	Measurement Value
MOS:	Metal Oxide Semiconductor
NDIR	Nondispersive infrared sensor
PCB	Printed Circuit Board
PPM	Parts Per Million
RH	Relative humidity expressed as a number between zero and

	one
RS	Sensor Resistance
RL	Load Resistance
Ro	Resistance in fresh air
SV	Stress Variable
Tdb	Dry bulb Temperature
THI	Temperature-Humidity Index
TV	Threshold Value
Twb	Wet bulb Temperature
Vc	voltage
WS	Wind Speed

1. INTRODUCTION

Several hazardous gases (CO_2, CH_4, NH_3, H_2S, and N_2O) are produced in livestock and poultry farms and released into the environment (Kılıç and Şimşek, 2009). The excessive accumulation of these gases inside farm structures such as barns and poultry houses may adversely affect the health and comfort of workers and farm animals (Yıldırım and Açar, 2023; Wu et al., 2020). In addition, the emission of these gases into the atmosphere can cause different environmental problems such as environmental pollution and global warming (Peterson and Mitloehner, 2021).

Air quality is very important for sustainable livestock farming because low air quality directly affects the health and comfort of animal health. The most important air quality parameter is thermal conditions in animal shelters. The thermal comfort of farm animals is described mainly by heat stress. Different numerical indexes have been proposed to quantify heat stress. The most widely used index describing the heat stress of farm animals is the temperature-humidity index (THI). Many equations have been derived to calculate the THI values. Cattle show optimal performance (thermoneutral range) within the normal range of THI values up to 70 (THI<70). Mild heat stress occurs in the case of 70 ≤THI < 74. Heat stress occurs in the case of 74 ≤ THI < 77, and severe heat stress occurs in the case of THI ≥77. Dairy cattle get stressed when the THI is above 72. The increase of THI from 67 to 78 reduced milk production by 21% and dry matter intake by 9.6%. The thermoneutral zone is usually accepted in the range of -0.5 to 20 °C and at a relative humidity in the range of 60% to 80%. (Kic, 2022). Heat stress is a major source of production losses in the dairy and beef industry (St-Pierre et al., 2003).

Microbial decomposition of organic nitrogen compounds, such as urea (mammals) or uric acid (poultry) in urine or as unabsorbed nutrients in animal feces, produces ammonia as a by-product (EPA, 2004). Livestock and poultry waste generates more than 60% of total atmospheric ammonia emissions in North America. Ammonia emissions from livestock (e.g., beef, dairy, pork, and poultry) are estimated to reach 2.67 million metric tons per year by 2030. Laying hens and broilers are one of the largest contributors to atmospheric ammonia emissions in the United States (Bist et al., 2023). High ammonia concentrations (e.g., >25 ppm) can cause discomfort in animals and workers by irritating the mucosa (eyes and respiratory tract), increasing susceptibility to respiratory disorders, and also affecting food intake, food conversion rate, and growth rate (Bist et al., 2023). Ammonia reacts with sulfur dioxide and nitrogen oxides forming aerosols which are ammonium nitrate and ammonium bisulfate. These aerosols are PM2.5 or particulate matter less than 2.5 microns in size. They can cause health problems including asthma, lung cancer, cardiovascular issues, birth defects, and premature death in humans (Wikipedia, 2024).

Some of the gases emitted from animal housings are greenhouse gases (GHGs) which induce global warming; one of the most urgent environmental issues. Livestock production accounts for 14.5 percent of world greenhouse gas emissions. Methane (CH_4), nitrous oxide (N_2O), and carbon dioxide (CO_2) are the three major GHGs emitted from agri-food systems. The gases produced by ruminant rumen microorganisms during feed fermentation are carbon dioxide, methane, and ammonia, with small amounts of hydrogen, hydrogen sulfide, carbon monoxide, and other gases. These gases approximately consist of 74.4% carbon dioxide and 17.3% methane (Ma et al., 2024). The most common source of greenhouse gases related to animal farming is enteric methane emissions from ruminant production, accounting for 46 percent of dairy and 55 percent of small ruminant production of total CO_2e emissions. Worldwide ruminant production is estimated to release between 80 and 95 million tonnes of CH_4 annually (Bačėninaitė et al., 2022). Methane is a greenhouse gas emitted from both natural and anthropogenic sources. Its impact on climate is 28–36 times stronger than that of carbon dioxide on a 100-year time scale (IPCC,2014). The global average estimation of GHG emissions per kilogram of milk and related milk products is 2.4 kg CO_2e. Methane, nitrous oxide and carbon dioxide account for about 52 percent, 27 percent, and 21 percent of GHG emissions generated from the dairy sector in developed countries, respectively. Nitrous oxide emissions increase to 38 percent while carbon dioxide emissions decrease to 10 percent in developing countries (Anonymous, 2010a). Climate change caused by global warming affects dairy farming directly, such as through effects on the performance and welfare of cows, or indirectly, such as through effects on the quantity and quality of feed production. (FAO and GDP, 2018). Ruminant CH_4 production is influenced by various factors including level of feed intake, type and quality of feeds, energy consumption, animal size, growth rate, level of production, and environmental temperature. Dairy cows can produce from 151 to 497 g of methane per day. Lactating cows, dry cows, and heifers produce 354 g, 269 g, and 223 g of methane per day, respectively. The average daily methane production range from 161 g to 323 g in beef cattle. Mature beef cows emit methane approximately from 240 g to 396 g per day (Broucek, 2014). A 700 kg cow with an annual milk yield of 10,000 kg is estimated to emit 4.7 t CO_2 per year. A simultaneous increase in CO_2 production per unit of time was observed with increasing food intake and performance (Jentsch et al., 2009).

Indoor air conditions of animal housings must be continuously assessed by automatic monitoring systems (Chen and Chen, 2019). These systems may have various sensors, a printed circuit board (PCB), a microcontroller, a power source, a wireless transmitter and receiver, a data storage unit, and an electronic equipment enclosure box. The temperature and humidity of the indoor air should be measured at regular intervals throughout the day to assess heat stress experienced by animals in barns (Kic, 2022). The accumulation of hazardous gases in animal housing also adversely affects the comfort and productivity of animals. Techniques for measuring the concentration of greenhouse and hazardous gases encompass a range of advanced methods. Electrochemical monitoring devices rely on redox reactions and electrodes, while infrared-based instruments, such as Fourier transform infrared (FTIR) spectrometers and non-dispersive infrared (NDIR) sensors, detect gases through absorption spectra. Laser-based detectors, including handheld laser methane detectors (LMD) and tunable diode laser absorption spectroscopy (TDLAS), operate on the principle of spectral absorption between lasers and gas molecules. Gas chromatography (GC) differentiates substances by their varying speeds as they travel through the column in the gas phase. Additionally, advanced remote sensing technologies using aircraft, drones, or satellites equipped with short-wave infrared (SWIR) cameras provide sophisticated methods for monitoring gas concentrations (Ma et al., 2024).

The aim of this thesis project is to develop a new air quality monitoring system consisting of various gas sensors and a temperature/relative humidity sensor to evaluate air quality and animal comfort in animal shelters.

2. LITERATURE REVIEW

Heat stress can be described as the inverse effect of excessive air temperature and relative humidity values on animal metabolism and behavior (Lutsko, N. J., 2021). Cows are unable to evaporate moisture from their skin and respiratory system effectively, which can reduce their ability to cool down under heat stress. The animals under heat stress change their feeding activities and mobility. Different numerical indexes have quantified heat stress. The most widely used indices describing the heat stress of farm animals is the temperature-humidity index (THI). Many equations have been derived to calculate the THI values.

$$THI1 = (1.8 \times T_{db} + 32) - [(0.55 - 0.0055 \times RH) \times (1.8 \times T_{db} - 26.8)] \quad (1)$$

$$THI2 = T_{db} + 0.36 \times T_{dp} + 41.2 \quad (2)$$

$$THI3 = (0.35 \times T_{db} + 0.65 \times T_{wb}) \times 1.8 + 32 \quad (3)$$

$$THI4 = (0.55 \times T_{db} + 0.2 \times T_{dp}) \times 1.8 + 32 + 17.5 \quad (4)$$

$$THI5 = (0.15 \times T_{db} + 0.85 \times T_{wb}) \times 1.8 + 32 \quad (5)$$

$$THI6 = [0.4 \times (Tdb + Twb)] \times 1.8 + 32 + 15 \quad (6)$$

$$THI7 = (T_{db} + T_{wb}) \times 0.72 + 40.6 \quad (7)$$

$$THI8 = (0.8 \times T_{db}) + [(\frac{RH}{100}) \times (T_{db} - 14.4)] + 46. \quad (8)$$

Where;

Tdb: dry bulb Temperature (°C)

THI: Temperature-Humidity Index ,

Twb: wet bulb Temperature (°C)

RH: Relative humidity expressed as a number between zero and one (Dikmen and Hamsen, 2009)

A rise in the temperature-humidity index (THI) results in reduced resting time and elevated respiration rates in dairy cows. Approximately 50% of the data indicates that cows are nearing distress when the THI is just below the heat stress threshold of 72. Consequently, a high THI is linked to adverse behavioral changes in cows. The heat stress threshold for dairy cows is generally identified at a temperature-humidity index (THI) of 72 or higher. However, signs of heat stress may begin to appear at lower THI values, particularly in the 60 to 72 range. This indicates that cows may already be suffering from heat conditions at THI levels slightly below this threshold. (Lovarelli et al., 2020).

Temperature and humidity conditions have been evaluted in 9 Canadian dairy farms, revealing that naturally ventilated barns exhibit a linear relationship between indoor and outdoor temperature-humidity index (THI), whereas mechanically ventilated barns show a nonlinear relationship; it emphasizes the importance of adapting thermal stress management recommendations according to barn design, noting that a THI threshold of 68 in Holstein dairy cows leads to a milk production decrease of 2.2 kg per day for every 24 hours at this THI, with thermotolerance influence by factors such as age, lactation stage, diet, thermal stress management, previous climate exposure, reproductive stage, parity, housing conditions, latitude, health status, and social ranking, highlighting the crucial roles of acclimatization and genetic adaptation. Nearby weather data (≤50 km) are more accurate for estimating barn conditions. (VanderZaag et al., 2023).

The research investigated hourly and daily indoor and outdoor environmental conditions across various farms, encompassing both naturally and mechanically ventilated barns. It compared on-site conditions with those recorded on the farm, at weather stations located up to 125 km away, and from NASA Power data. The Temperature-Humidity Index (THI) measured inside dairy barns was closely aligned with THI values observed outside the barns. In naturally ventilated barns featuring metal roofs and no sprinklers, a linear relationship with a slope below 1 was identified for hourly and daily averages. This suggested that indoor THI levels exceeded outdoor THI more at lower values but equalized as THI increased. Mechanically ventilated barns exhibited nonlinear patterns, with indoor THI surpassing outdoor THI at lower levels and converging at higher levels. During the evening and nighttime, the THI inside barns was notably higher due to factors such as reduced wind speeds and retained latent heat. Eight regression models were developed to forecast barn conditions based on external environmental data, accounting for variations in barn design and management practices. The findings underscore the importance of tailoring heat stress guidelines to barn designs and selecting meteorological data that align with specific research objectives (VanderZaag et al., 2023).

Climate change, a key aspect of global warming, is expected to significantly influence the productivity of farm animals and have far-reaching effects on livestock production globally. As temperatures rise, farm animals face increased vulnerability to heat stress. To mitigate the effects of climate change on livestock, it is essential to develop a deeper understanding of how animals respond to environmental changes (Nardone et al., 2010). The heat stress occurrences at various air temperature and relative humidity combinations for cattle are shown in Table 1.

Table 1: Heat stress occurrences at different temperatures and relative humidity values for cattle (Anonymous, 2013a).

Ambient Air Temp	Relative Humidity(%)					
°c	20	30	40	50	60	70
37.8	26	29	30	31	33	34
36.7	26	28	29	31	32	33
35.6	26	27	28	30	31	32
34.4	26	27	28	29	31	32
33.3	25	26	27	28	29	30
32.2	25	26	26	27	28	29
31.1	24	24	26	27	27	28
30	23	24	25	26	27	27
28.9	22	23	24	25	26	27
27.8	22	23	23	24	25	26
26.7	21	22	23	23	24	24
25.6	20	21	22	23	23	24
24.4	19	21	21	22	22	23
Livestock Safety Index (°c)	Normal<23	Alert 24-25.5		Danger 26-28	Emergency>29	

Air quality plays a vital role in environmental health, impacting animals wellness. Other elements of air quality are the concentration of gases and particulate matter. Gas concentration indicates the presence of specific gases in the atmosphere, usually quantified in parts per million (ppm) or parts per billion (ppb). Typical gases of concern include carbon monoxide (CO), carbone dioxide sulfur dioxide (SO_2), nitrogen oxides (NO_x), and ozone (O_3). Air particulate matter (PM) is often categorized based on its diameter: PM10 and PM2.5 (Sonwani et al., 2022). Both gas concentration and particulate matter have significant impacts on health and the environment. High levels of pollutants can lead to respiratory and cardiovascular diseases, as well as contribute to climate change. Monitoring and regulating these components are essential for maintaining air quality and protecting public health.

Emissions of greenhouse gases and other pollutants from livestock housing are reviewed, with a focus on measurement methods and environmental impacts. The study includes results from the APECAB project, which quantifies emissions of gases such as ammonia (NH_3) and hydrogen sulfide (H_2S) in various barns. The importance of waste management and husbandry practices to reduce emissions and improve air quality is highlighted. Major measurement errors include diurnal and seasonal variations, leaks in the sampling system, and condensation in the sampling lines. The study findings indicate that ammonia (NH_3) concentrations in exhaust air vary between 5 and 35 ppm, while ambient air levels are much lower, around 0.3 ppm. Carbon dioxide (CO_2) is highlighted as an important gas to monitor, and methane (CH_4) concentrations range from 5 to 60 ppm, especially during slurry pit leaching events (Heber et al., 2006).

Ammonia (NH_3) concentrations often reach potentially dangerous levels exceeding 20 ppm for more than half of the production cycle. At the end of the production cycle, ammonia production rates decrease significantly. The barns use negative pressure ventilation systems, with fans located along one wall. Fresh air is introduced into the barns through slotted air inlets. One barn was equipped with a fan-driven air heater for additional air mixing, while the second barn relied solely on inlet air velocities for mixing (Glennon et al., 1989).

A methodology was developed to evaluate sampling design in long-term air quality studies and to evaluate the design of a gas sampling system on two commercial farms. This aimed to understand spatial and temporal variations in air pollutant concentrations. Gas concentrations, particularly CO_2, increased gradually from the west to the east end of the barns, following the direction of manure movement. Concentration variations were more pronounced between different areas of the barns than between the north and south sides. Significant differences in concentration were observed, with maximum values reaching up to 101.2 ppm for NH_3 in some areas. Temperature and humidity conditions were measured using portable sensors fixed at specific locations in the barns, including at the fans. Indoor temperature was calculated as the average of measurements taken at several fans, while relative humidity was measured at a fixed location. The measurements were carried out under quasi-steady-state conditions to minimize temporal variations (Chai et al., 2010).

A cross-sectional study involving 428 calves across 60 farms found that indoor air quality factors, such as average temperature, ammonia levels, and air velocities exceeding 0.8 m/s, were linked to pulmonary consolidations. The study reported that 41.1% of the calves exhibited pulmonary consolidations measuring 1 cm or larger. Air quality parameters were assessed using equipment positioned at the calves' breathing height within their enclosures. Temperature, relative humidity, and ammonia levels were continuously monitored over a 24-hour period, while spot measurements of air velocity, CO_2, and ammonia were taken at multiple locations within each enclosure. All measurement instruments were pre-calibrated by the manufacturer to ensure accuracy. The average air volume per calf across the farms was 24.8 ± 50.9 m^3, with values ranging from 1.9 to 377.2 m^3. The findings underscore the critical role of monitoring indoor air quality parameters to mitigate respiratory diseases in calves (Van Leenen et al., 2020).

The findings demonstrated that the applied methodology effectively quantifies methane concentrations with minimal RMSE while mitigating the influence of $H_2O(g)$, a critical factor for the practical use of chemical sensors. Prior to training the PLSR regression model, the dataset was standardized using Z-transformation. This process involved subtracting the mean of all data points from each individual data point and dividing the result by the corresponding standard deviation. Standardization is crucial to ensure all variables contribute equally to the analysis, preventing larger-scale variables from overshadowing others, which could result in biased or unreliable outcomes (Domènech-Gil et al., 2023).

In 2007, milk production resulted in the emission of 553 million tonnes of greenhouse gases (GHG), equivalent to 1,328 million tonnes of CO_2-equivalent (CO_2-eq). Each kilogram of dairy product was associated with 2.4 kg of CO_2-eq emissions, accounting for 2.7% of global anthropogenic emissions. Additionally, meat production from dairy cows and bulls generated 10 million tonnes of GHG, equivalent to 151 million tonnes of CO_2-eq, with an emission ratio of 15.6 kg of CO_2-eq per kilogram of meat, representing 0.3% of total emissions. Finally, meat from fattened calves contributed to 24 million tonnes of GHG, corresponding to 490 million tonnes of CO_2-eq, with an impact of 20.2 kg of CO_2-eq per kilogram of meat, or 1.0% of anthropogenic emissions (Mostert, 2018).

Machine learning techniques are frequently utilized to enhance the utility of gas sensor data. Models of various complexities, accounting for fluctuations in temperature and humidity, were trained using over 50,000 calibration data points. These data points spanned methane concentrations from 0 to 200 ppm, temperatures from 5 to 30 °C, and relative humidities from 40% to 80%. The final selected model achieved a root-mean-square error of 5.1 ppm and an R-squared value of 0.997. This success highlights the NGM2611-E13 sensor's capability to accurately measure methane concentrations below 200 ppm. Regression machine learning techniques can calibrate gas sensor outputs under varying environmental conditions, such as target gas concentration, temperature, and humidity, thereby compensating for long-term sensor drift. Various nonlinear models, incorporating sensor responses to different methane concentrations, temperatures, and humidities—some with interaction terms—were developed and tested. These models are instrumental in calibrating low-cost methane sensors (Mitchell et al., 2024).

Affordable methods are proposed to monitor air pollution. Low-cost sensors calibrated by a machine learning model (LinearForestRegressor) are used in this study. The integration of low-cost stations with remote data transmission modules, such as LoRaWAN, allows real-time uploading of air quality data to a centralized server. This facilitates access, control, and processing of data for end users, thereby improving air quality monitoring and management. Furthermore, it helps regulators and researchers to make informed decisions based on up-to-date and high-resolution data. The results give us a high accuracy with R^2 ranging from 0.8781 to 0.9827 for CO_2 and 0.7312 to 0.9410 for CH_4 (Biagi et al., 2024).

The document discusses the long-term reliability and performance of the Figaro TGS 2600 solid-state methane sensor. The study employs various statistical methods, including linear models and artificial neural networks, to assess the sensor's performance. Additionally, it highlights the challenges faced in extreme arctic conditions and suggests areas for future research to improve sensor accuracy, particularly concerning temperature and humidity effects. The Figaro TGS 2600 solid-state methane sensor demonstrates long-term reliability in measuring ambient methane levels in low-Arctic conditions. The sensor's performance was assessed using various indicators such as bias, stability, variability, and correlation with reference measurements. While the sensor showed good overall performance, the study suggests that future improvements could focus on enhancing the correction models for temperature and humidity effects, particularly in extreme conditions. The findings underscore the potential of low-cost sensors for effective atmospheric methane monitoring, although they also highlight the need for careful calibration and validation against reference instruments (Eugster et al., 2020).

The Figaro TGS2600 sensor was designed to detect methane concentrations across two different environments. It underwent a multi-point calibration process, including testing at a wastewater treatment facility using a multigas analyzer (Gasera One Pulse). Calibration of the low-cost sensor was performed by correlating its readings with those of the reference device. To reduce the influence of temperature and relative humidity on the sensor’s signal, these variables were also measured, and an active ventilation system was implemented to enhance performance. The low-cost system demonstrated the ability to reliably detect low methane concentrations, providing consistent spatial and temporal patterns in both environments. Its strong performance under various environmental conditions highlights its potential as a cost-effective solution for screening and monitoring systems (Furst et al., 2021).

The River Runner is an innovative, low-cost sensor prototype designed for continuous monitoring of dissolved greenhouse gases (GHGs) in submerged environments. It operates by utilizing a confined gas space that equilibrates with the water phase through a single-layer polytetrafluoroethylene (PTFE) membrane. The sensors are capable of measuring CO_2 concentrations ranging from 400 to 10,000 ppm and CH_4 concentrations from 2 to 50 ppm, with respective accuracies of ±58 ppm and ±3 ppm. This prototype successfully captured diurnal variations in dissolved CO_2 levels in a natural stream and was calibrated for in situ CH_4 measurements at concentrations between 0.01 and 0.3 μmol L^{-1}. Underwater, the CH_4 molar fraction within the prototype head was measured with an accuracy of ±13 ppm for values ranging from 2 to 172 ppm. However, measurement errors for CH_4 underwater were higher compared to air measurements, particularly at concentrations below 10 ppm, where CH_4 levels were significantly overestimated. The study highlights the performance characteristics of low-cost sensors in submerged settings and provides calibration techniques to account for the effects of temperature and humidity on sensor readings. Additionally, detailed do-it-yourself guidelines are offered for constructing sensors capable of continuously measuring dissolved CO_2 and CH_4 underwater. The prototype operates independently of external power sources, making it a durable and economical tool for future environmental studies (Furst et al., 2021).

This study explores the potential of a low-cost methane (CH_4) gas sensor based on metal oxide technology for atmospheric methane monitoring. A custom sensor assembly was developed to power the sensor and its resistive heater, record ancillary temperature and relative humidity data, and manage sensor readout and data storage. Following calibration for methane concentration, temperature, and relative humidity, the sensor was able to estimate CH_4 levels in laboratory air over a 31-day period across a wide range of temperature and humidity conditions. The measurements exhibited a systematic error of -1.0 ppm and a variable error within ±1.7 ppm, with no significant drift observed in the CH_4 estimates. The findings suggest that accuracy could be further enhanced by optimizing the voltage regulator powering the sensor's heater and by compensating for differences in partial oxygen pressure between calibration and validation conditions. These enhancements could make the sensor assembly suitable for applications such as fence-line methane monitoring near fossil fuel extraction sites. In its current configuration, the assembly effectively detects fugitive methane emissions from equipment prone to leaks (Bossche et al., 2017).

The calibration method for the TGS2611-E00 sensor is based on a calibration curve based on the average linear response of CH_4 sensor versus change in CH_4 concentration. This calibration was carried out in a 7 L chamber with a range of 10 mL CH_4 at 1000 ppm, at different temperatures ranging from 10 to 35 °C (60-90% relative humidity). Every 5 minutes, 10 mL of CH_4 at 1000 ppm was injected into the chamber. The results were analyzed using JMP Pro and MATLAB software. Interestingly, the differential signal from the CH_4 sensor was less sensitive to temperature and exhibited a linear response ($R^2 = 0.98$; $p < 0.001$). To calibrate the AFC CH_4 sensor, it is recommended to do so individually due to variations in response slope between sensors. To obtain a general calibration line, it is recommended to calibrate at least five CH_4 sensors to guarantee statistical representativeness (Thanh et al., 2020).

The TGS2600 sensor was calibrated by operating it alongside a high-precision instrument, the Ultra-portable Greenhouse Gas Analyzer (UGGA) from Los Gatos Research. This approach is chosen because the TGS2600 does not accurately measure CH_4 under low relative humidity conditions (<40%), making in-cylinder reference gas calibration challenging. Standard calibration gases cannot be used for the TGS2600 due to their low humidity. Instead, the most accurate calibration involves running the TGS2600 alongside the UGGA for a specific duration. However, the TGS 2600 is susceptible to drifting, with daily variations averaging 0.002 ppm. Frequent calibration is recommended—ideally every two months—to maintain accuracy. Despite these challenges, the TGS2600 effectively measured CH_4 mixing ratios within 0.01 ppm compared to the UGGA reference instrument over three months. It operated autonomously using a 35 Ah lead-acid battery for up to seven days, with data logged on an SD card. This demonstrates the feasibility of deploying TGS2600 sensors in a network to assess changes in CH_4 emissions, contingent upon regular calibration against a high-precision standard for reliable comparisons (Riddick et al., 2020).

This paper explores the monitoring of ammonia concentrations using an affordable electronic device based on the Arduino platform. The system utilizes the MQ-137 ammonia sensor integrated with the Croduino Basic 2 board. The sensor operates on a metal oxide (SnO_2) as its sensitive material, where variations in ammonia concentration result in changes in electrical resistance. These resistance changes are measured and used to estimate ammonia levels. Four experiments were conducted within a controlled environment, with ammonia concentrations ranging from 0 to 500 ppm. To ensure accuracy and test repeatability, measurements from the low-cost device were compared to those obtained from a professional instrument, the Geotech GA5000 gas analyzer. The measurement error for the low-cost device was determined by referencing the sensor datasheet alongside experimental data. Following calibration, the ammonia concentrations recorded by the low-cost device closely matched those of the professional analyzer. The Arduino platform has become widely used due to its accessibility, affordability, ease of learning, and extensive documentation. This paper specifically focuses on monitoring ammonia levels during the photocatalysis process using the MQ-137 sensor. The MQ-137 sensor has demonstrated versatility in scientific applications, such as classifying spoiled meat, building an electronic nose for saffron aroma characterization, and detecting seasonal allergic rhinitis through exhaled breath analysis (Petric et al., 2019).

This research examines indoor ammonia (NH_3) concentrations in the air within a free-stall barn, highlighting how seasonal and weather variations influence the results. A strong correlation ($P<0.01$) was observed between ammonia levels and factors such as temperature, relative humidity, and air movement inside the barn. The lowest ammonia concentration (0.0 ppm) occurred during summer, when high temperatures, low humidity, and efficient ventilation enhanced air exchange. Conversely, the highest concentration (8.0 ppm) was recorded in winter during extreme cold, as limited ventilation restricted air circulation. Nighttime measurements typically revealed peak ammonia levels, attributed to higher relative humidity and reduced air velocities. The study concluded that annual average ammonia concentrations remained significantly below thresholds harmful to animals and humans. Ammonia emissions from livestock production are a key contributor to air pollution, linked to environmental issues such as acid rain, eutrophication of water bodies, soil acidification, and loss of plant biodiversity. When combined with other pollutants, ammonia can exacerbate respiratory and cardiovascular health issues. Elevated ammonia levels in barns can irritate animal skin, cause tissue inflammation, weaken immunity, increase disease susceptibility, and lower milk production. The primary sources of ammonia in barns include manure, liquid manure, slurry, bedding materials, and cattle feed (Herbut et al., 2014).

The online gas monitoring tool (OTICE) utilizes a wireless sensor network featuring low-cost sensors to monitor gas concentrations and climate variables, enabling scalable implementation across multiple barns. Researchers assessed the accuracy of sensors for CO_2,

NH_3, and CH_4 under controlled laboratory conditions and within a dairy barn in Germany. Over the measurement period, the average concentration levels recorded by the low-cost sensors showed strong agreement with the reference system, with relative deviations below 7% for all three gases. However, peak deviations reached up to 32% for CO_2, 67% for NH_3, and 65% for CH_4.The promising results, particularly for NH_3 and CO_2, highlight the potential of this low-cost system as a practical solution for monitoring relative NH_3 emissions and calculating air exchange rates in naturally ventilated barns (Janke et al., 2023).

An Ogawa passive sampler (Ogawa) and a passive flux sampler (PFS) were used to measure NH_3 concentrations in naturally ventilated (NV) dairy barns. These samplers were placed near sampling ports of a photoacoustic infrared multigas spectroscope (INNOVA) within an NV dairy barn. A deployment period of three days was found suitable for both passive sampling methods. Statistically significant correlations were observed between NH_3 concentrations measured by the passive samplers and those recorded by the INNOVA ($r = 0.93$ for Ogawa and $r = 0.88$ for PFS). Compared to the reference measurements, the Ogawa sampler overestimated NH_3 concentrations by approximately 14%, while the PFS underestimated them by about 41%. After calibration, NH_3 emission factors per animal unit (20.6–21.2 g d^{-1} AU^{-1}) determined by the passive samplers aligned closely with those obtained using the reference method and fell within the range reported in existing literature. Atmospheric ammonia contributes to the formation of fine particulate matter and can lead to soil acidification and surface water eutrophication. Measuring NH_3 emissions from livestock barns is essential for evaluating emission reduction strategies, validating emission models, and generating accurate emissions inventories. NH_3 measurement devices are typically categorized into three types: rapidly responding sensors for time-series data, cumulative-concentration devices for time-averaged values, and instantaneous devices for single-point measurements. While rapidly responding sensors are costly, they are invaluable for capturing the dynamics of gas emissions (Wang et al., 2016).

This study focuses on developing an IoT-based platform to monitor air quality in various indoor environments, including homes, offices, schools, hospitals, and shopping centers. The system utilizes Raspberry Pi 3 control boards along with sensors for temperature and humidity, leveraging web-based data to evaluate indoor air quality. Sensor readings from the indoor environment are transmitted to the control board, which processes the data to assess air quality levels. The real-time monitoring system provides immediate feedback on indoor air conditions, enabling more effective management of air quality. Additionally, a mobile application has been developed to allow users to monitor air quality remotely in real-time. This research underscores the significant role of IoT technology in enhancing indoor air quality monitoring systems, addressing challenges faced by individuals who spend the majority of their time indoors. By integrating IoT technology, the study aims to improve the accuracy and efficiency of indoor air quality monitoring, helping to mitigate the adverse impacts of air pollution on human health, the climate, and ecosystems (Ucgun et al., 2020).

The study investigates the concentration gradients of ammoniac (NH_3), carbon dioxide (CO_2), and methane (CH_4) in a naturally ventilated building. Measurements were taken at different heights (0.5 m, 1.5 m, 2.7 m) and mixture ratios were analyzed. Results showed significant differences in gas concentrations based on the height of the building. All gas was primarily concentrated at the maximum height (2.7 m) during low wind events, while concentrations varied at higher wind speeds. The speed of wind significantly influences gas concentrations, with significant increases at low wind speeds, up to +105.1% relative to the base line. However, these increases are less at higher wind speeds, indicating that higher wind speeds lead to a dilution of gas concentrations. The recommended height for gas measurements is 1.5 m, as it ensures stable mixture ratios and minimizes animal influences on concentrations. The position of sensors is crucial for precise measurements (Sahu et al., 2023).

A study was conducted on low-cost CO_2 and CH_4 sensors to determine their detection limits, precision, and exactitude. The tests involved a gas mixture chamber for precise measurements. The NDIR (K-30, Gascard) sensors showed good performance, while the chemiresistive (MQ-4) sensors had higher detection limits. The results serve as a reference for the development of low-cost sensors. The sensors were tested for their accuracy and exactness over a 20-30 hour period at a known gas concentration, usually around 400 ppm for CO_2. A high-quality reference device was used to prepare known gas mixtures for accurate and reproducible measurements. The results were analyzed using linear regressions and other statistical methods. The detection limits varied, with Gascard, K-30, and Telaire having lower detection limits, while Dynament had higher limits. For CH_4, chemiresistive sensors had detection limits exceeding 100 ppm, which does not meet environmental surveillance requirements. NDIR sensors showed better accuracy and exactitude at concentrations close to typical atmospheric levels (400 ppm for CO_2 and less than 2 ppm for CH_4) (Honeycutt et al., 2019).

The paper presents a simple method for calibrating the DHT22 relative humidity sensor, specifically adapted to tropical climates, using an Arduino-based data acquisition system. The results show that calibration improves the accuracy of measurements, involving errors compared to uncalibrated data. The study highlights the importance of proper calibration to ensure reliable readings in tropical environments (Koester et al., 2019).

The use of MOx sensors for the detection of low methane concentrations faces several major challenges, including ambient temperature and humidity fluctuations that impact their reliability. To overcome these obstacles in practical applications, accurate sensor calibration and implementation of advanced algorithms are essential. The study highlighted the TGS2611-C00, TGS2611-E00 and MQ4 sensors as promising for detecting trace amounts of methane, despite difficulties encountered with environmental variations. These results indicate that these sensors can be suitable for low concentration applications, but require adjustments to optimize their performance under varying conditions (Furuta et al., 2022).

Harmful gases concentrations and oxygen concentrations in animal housing must be monitored with appropriate measurement equipment. However, much of the equipment is expensive and requires periodic re-calibration. Farmers need to have evidence at their fingertips like knowing harmful gas levels through low-cost monitoring systems, presented in a clear and understandable way, so they will see how they can and should contribute to animal comfort. Therefore, an inexpensive new online measurement system, suitable for use in animal housings to monitor the air quality needs to be developed. Ammonia is not a greenhouse gas but a main harmful gas that causes environmental deterioration via acid rain and is emitted from animal housings (Anonymous, 2018a).

3. MATERIALS AND METHODS

Research was conducted to determine available wireless indoor environmental sensors based on a certain number of criteria such as measuring capacity under difficult conditions, concentration ranges, internet connectivity, ease of access to measured data, on the availability of hardware parts including sensors. The measurement ranges, sensitivities, environmental factors and costs of gas sensors vary according to their detection principles. Two different sensor types were considered for each gas at the beginning of this study. Methane and ammonia gas concentrations are often low (less than 50 ppm) in open cow barns (Ngwabie et al., 2009; Wu et al., 2016). These values can be very high in completely closed barns. However, barns are not completely closed on many dairy farms all over the world.

This chapter provides a detailed explanation of the various steps and procedures undertaken throughout this thesis. The following diagram offers a concise overview of the methodology employed (Figure1).

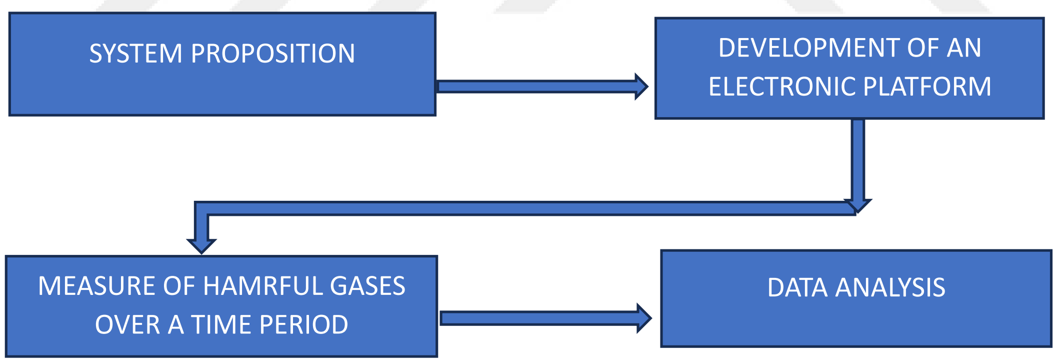

Figure 1 : An overview of the methodological approach followed in this thesis.

These steps are explained in more detail in the following subsections.

3.1. Design And Manufacturing Of Air Quality Monitoring System

3.1.1. Hardwares design

The electronic architecture of air quality monitoring system is given in Figure 2

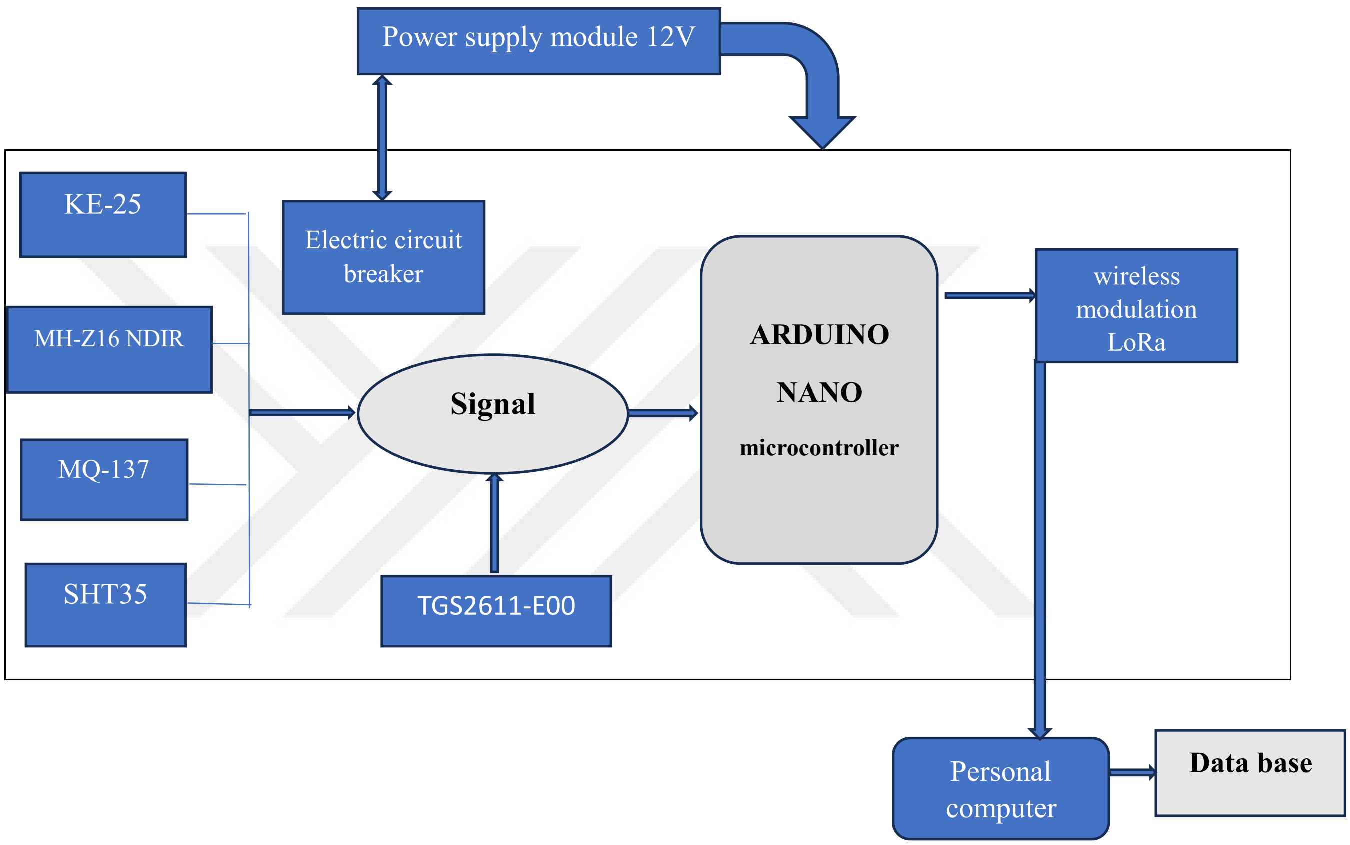

Figure 2: The electronic architecture of air quality monitoring system.

The electronic components air quality monitoring system includes a main control microcontroller, ARDUINO NANO, a storage unit, a wireless modulation LoRa, an oxygen sensor (KE-25), a sensor for gas methane (TGS-2611), a carbon dioxide sensor (MH-Z16 NDIR), an evaluation module (EM7162), an ammonia sensor module MQ-137, an temperature humidity sensor (SHT35), an amplifier LM358, an electronic card, a clock circuit, a control circuit (PCB) .

After some tests of different types of microcontrollers, ARDUINO NANO has been chosen. The selected microcontroller runs under low power consumption. It has strong ability of data handling capacity. The best microcontroller to use for the online system can be ESP32 (anonymous, 2021b). But it didn't work well with one of the sensors selected for the system during the programming. ARDUINO NANO performed with all the sensors. It features 8 analog input pins, 22 digital I/O pins, and supports an input voltage range of approximately 7 to 12V. Each I/O pin can handle a DC current of up to 20 mA (Figure 3).

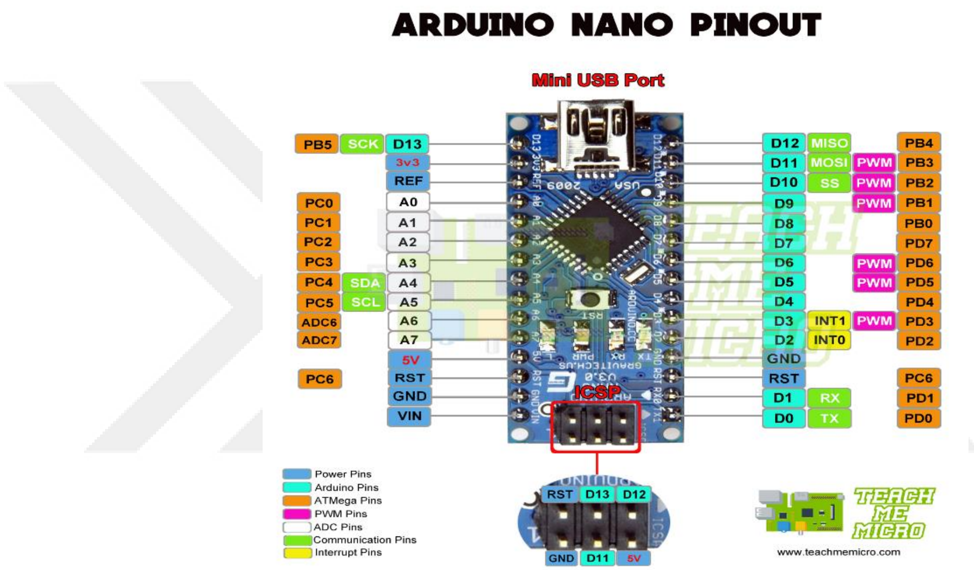

Figure 3: Logout of ARDUINO NANO microcontroller

An EC ammonia sensor was selected at the beginning. However, no signal could be received from the selected EC sensor. They were much more adversely affected by atmospheric conditions. Therefore, it was decided not to use EC sensors. MQ 137 sensors are frequently used in the measurement of ammonia gas (Petric et al., 2019). It was decided to use the MQ137 ammonia sensor in the measurement of ammonia concentration. MQ 137 is manufactured by Winsen Electronics and has a range of 10 to 1000 ppm and an input voltage of 5.0V (Figure 4). A regression analysis might be done to calibrate the accuracy of this sensor (Anonymous, 2015).

Figure 4: MQ-137 ammonia sensor

Low-cost oxygen sensors are the most difficult to find. Two different oxygen sensors were considered in this study. The sensors under consideration include the O2-A3, O2-A1, KE-25, and KE-50. The O2-A3 and O2-A1 sensors are cost-effective and energy-efficient, requiring no warm-up time, making them seemingly more practical options compared to the KE-25 and KE-50. However, a significant limitation of the O2-A3 and O2-A1 sensors is their nanoampere (nA) output, which necessitates the integration of an external amplifier circuit. This additional requirement increases the overall system cost. Consequently, the KE-25 sensor from FIGARO was selected for implementation in this project due to its practicality and cost-effectiveness (Figure 5),

Figure 5: KE-25 oxygen sensor

KE-25 oxygen sensor requires on external amplifier circuit since it produces outputs at the levels of nano-ampere (nA)

The LM358 used at this study is a dual-channel operational amplifier that can operate with a single power supply. It's designed to work with a wide range of supply voltages, from ±1.5V to ±16V for op-amp applications, or from 3V to 32V when used as a comparator. It's commonly used in various electronic projects due to its low power consumption and cost-effectiveness (Figure 6).

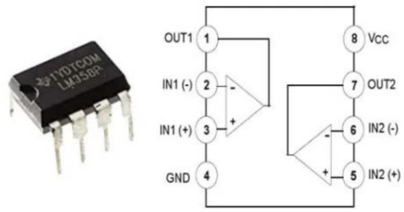

Figure 6: LM358 amplifier

Two different CO_2 sensors were considered in this study. They are K30 or MH-Z16 NDIR. The K30 carbon dioxide sensor was replaced due to its unavailability within Turkish territory and the prohibitive shipping costs associated with importing the sensor from the United States. To address this, 15 electronic purchasing platforms in Türkiye were reviewed. During this process, the Turkish distributor FIGARO was identified through an online search. Subsequently, the MH-Z16 NDIR sensor from FIGARO was selected, as its specifications closely aligned with typical concentration ranges required for the intended application (Figure 7).

Figure 7: Winsen MH-Z16 NDIR infrared CO_2 gas module

Two different types of methane sensors were initially considered. The first sensor was a NDIR sensor (MH 440 D). The sensor failed to produce any detectable signal, leading to the conclusion that NDIR methane sensors are not suitable for detecting very low methane concentrations (0–50 ppm). A market analysis revealed the availability of various MQ methane sensors, and a review of the literature identified the TGS 2611-E00 methane sensor, manufactured by FIGARO, as suitable for low methane concentrations, particularly for monitoring atmospheric methane levels (Domènech-Gil et al., 2023; Figaro, 2013). This sensor, equipped with a specialized filter, exhibits higher sensitivity to interference from other gases. Consequently, the Figaro NGM2611-E13 gas module, which incorporates the TGS 2611-E00 sensor, was selected for this project (Figaro, 2022). Preliminary tests conducted under current atmospheric conditions demonstrated that the gas module successfully generated an electrical signal, confirming its applicability for the intended purpose.

The TGS2611 is a semiconductor-type methane gas sensor known for its low power consumption. It offers very high sensitivity to methane gas, making it suitable for detecting low concentrations. The sensor has a long operational life, providing reliable and continuous methane gas detection and requires only 56 mA for heater current, contributing to its energy efficiency. it is also compact in size and housed in a standard TO-5 package, making it suitable for various applications (Figure 8).

The selection of specific sensor models was made in consultation with sensor company representatives, considering factors such as methane (CH_4) specificity, adequate sensitivity for the intended applications, cost, and power consumption. For methane gas measurement, the NDIR methane sensor and the MQ methane sensor were chosen. However, no electrical signal was detected from the supplied NDIR sensor, leading to the conclusion that these sensors are ineffective at detecting very low methane concentrations (0-50 ppm). Among the various MQ methane sensors available on the market, literature research identified the TGS2611-E00 sensor, developed by the FIGARO company, as suitable for detecting low methane concentrations, particularly for monitoring atmospheric methane levels (Domènech-Gil et al., 2023). The performance of the CH_4 sensor was evaluated based on its response to methane concentration, temperature, and relative humidity (RH) in a controlled environment. The impact of hydrogen sulfide (H_2S), a potential interference gas from certain sediments, was also examined. The TGS2611-E00 sensor features a filter designed to minimize the influence of interfering gases, such as ethanol, enhancing its selectivity for CH_4. Consequently, the NGM2611-E13 gas module was selected for methane concentration measurements in the project (Figaro, 2013).

Figure 8 : NGM2611-E13 methane gas module

SHT35 air temperature and relative humidity sensor is one of the temperature sensors often used in many IoT projects. The SHT35 is a digital temperature and humidity sensor that is part of Sensirion's SHT3x series (Figure 9). Known for its high accuracy, here are some of its main features: humidity accuracy: ±1.5%RH (0-80%RH); temperature accuracy: ±0.1°C (20-60°C) and ±0.2°C (-40-90°C); Interfaces: I²C, analog output; voltage range: 2.15 to 5.5 V. This highly sensitive, energy-efficient sensor offers excellent stability and a low response time. The sensor interfaces with the I2C port of an Arduino microcontroller, with the ARDUINO NANO being a compatible platform for integration. A detailed comparison of Sensirion's SHT sensors, as incorporated into DFRobot modules, is provided in the sensor's datasheet. Additionally, DFRobot offers an Arduino® library and a sample program to facilitate implementation.

Figure 9 : SHT35 Temperature and Humidity Sensor Waterproof Stainless Steel Probe

LoRa (from « long range ») is a proprietary physical radio communication technology. It utilizes spread spectrum modulation techniques inspired by chirp spread spectrum (CSS) technology (Anonymous, 2024b). A 433 MHz lora module (Figure 10) with a power of 1 W and a range of 10 km was used for wireless transmission of the gas measurement unit to the climate unit. A 40 dBi SMA 433 MHz antenna was attached to the module (Figure 10).

Figure 10 : 433 Mhz Lora Module with 10 km range

The SIM800L GSM/GPRS module used in this project is a compact GSM modem suitable for various IoT applications. This module enables functionalities similar to those of a standard mobile phone, including sending SMS messages, making calls, accessing the Internet through GPRS, and more (Figure 11) (Anonymous, 2024c).

Figure 11 : Sim800 Series Arduino Gsm Gprs Module (Simcom Sim800L)

3.1.2. Software Requirement

Programming language C++ used in this study is a highly popular programming language recognized for its efficiency, adaptability, and beginner-friendly nature. Its use of Object-Oriented Programming (OOP) enhances code structure and ensures optimized performance with minimal resource use. Development in C++ typically involves an Integrated Designed Environment (IDE) equipped with a text editor, compiler, and debugging tools, facilitating the creation of complex applications. (Anonymous, 2023). The Arduino IDE, an open-source platform, allows users to easily write, compile, and upload code to Arduino modules, making it an excellent starting point for beginners (Anonymous, 2018b). For circuit design, Fritzing software provides an open-source solution that enables users to prototype and transform their designs into permanent circuits (Anonymous, 2024d). EasyEDA software is an online tool for PCB design that simplifies the process of turning concepts into physical projects. In the realm of mechanical design, SOLIDWORKS software offers a comprehensive suite for 3D modeling, design validation, sustainable engineering, and data management, supporting the creation of fully integrated digital models (Anonymous, 2010b).

3.1.3. Preparation and Calibration of Sensors

The concentration of carbon dioxide (CO_2) in naturally ventilated dairy barns fluctuates depending on sensor placement and environmental factors. Research indicates that in areas with low wind speeds (below 3 m/s), the average CO_2 concentration ranged between 625–657 ppm at lower sampling heights (0.6 m) and increased to 648–700 ppm at the highest sampling height (2.7 m). In contrast, under high wind conditions (above 3 m/s), the CO_2 concentration followed a decreasing trend with height, with values dropping by up to 7.83% at the highest point compared to the baseline. This trend suggests that at higher wind speeds, CO_2 disperses more effectively, reducing accumulation at elevated heights. The variations in CO_2 concentration are attributed to differences in animal respiration, barn ventilation patterns, and mixing dynamics within the structure. The results highlight that sensor positioning significantly affects measurements, and an optimal placement strategy is necessary for accurate CO_2 monitoring (Sahu et al., 2023).

Enhancing sensor measurement accuracy requires consideration of various factors, including the calibration environment and implementation conditions. A controlled calibration chamber allows for safer detection of toxic gases such as carbon monoxide, carbon dioxide, and methane, with methods like fuzzy logic improving measurement reliability (Slamet W. et al., 2019). Metal oxide semiconductor (MOS) and electrochemical sensors offer advantages in terms of compact size, low power consumption, and cost-effectiveness, but additional measures are needed to optimize their outdoor performance (Mitchell et al., 2024). Therefore, it was decided to calibrate these sensors before use.

The MH-Z16 NDIR carbon dioxide sensor is pre-calibrated during manufacturing, while methane and ammonia sensor calibration is the primary focus of this study. The response of a metal oxide (MOx) sensor to methane concentrations is influenced by temperature (T) and relative humidity (RH). This research examines the calibration methodology, the reference measuring device (if applicable), and the reference gases used. Key factors considered include the gas concentration range for calibration, environmental conditions (temperature and humidity), preliminary preparations (such as sensor preheating), resistor values, calibration chamber setup, and sensor mounting. Additionally, the study evaluates the recommended calibration equation and its limitations concerning range, temperature, and humidity.

TGS2611-E00 methane sensors are factory-calibrated for the range of 500 to 10000 ppm at 20±2˚C and 65±5%RH) (Figure 12) (Figaro, 2013).

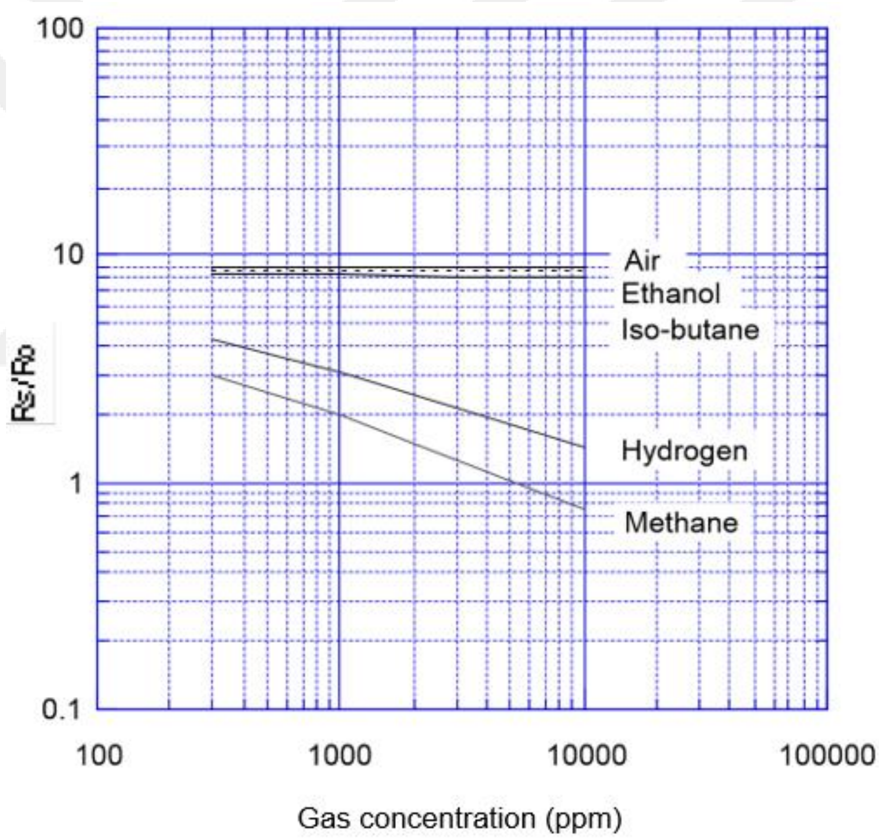

<u>Figure 12</u>: Calibration curve of Figaro TGS2611-E00 methane sensor

This sensor was normally calibrated for residential gas leakage detectors which require durability and resistance against interference gas. Therefore, it must be calibrated again to improve their accuracy, particularly by accounting for interactions between temperature, relative humidity, methane concentration, and sensor voltage output for methane concentrations that are lower than 500 ppm. Numerous studies reported the calibration of this sensor for lower methane concentrations. Encouragingly, many of these studies report a strong correlation between the calibrated sensor output and the actual methane concentration. In previous studies, single or multiple methane sensors were calibrated at the same time. It has been reported that sensors can give slightly different results for given actual gas concentrations. Therefore, experimental data from more than one gas sensor should be used in developing calibration models and determining their performances. Various nonlinear regression models tailored for calibration that can further enhance their performances for low methane concentrations have been proposed. The most accurate models were selected based on two prediction performance indicators: a high coefficient of determination (R^2), indicating a strong correlation between predicted and actual values, and a low root mean square error (RMSE), ensuring minimal deviation from true methane concentrations.

The gas concentration ranges used for calibration depend on the concentrations in the enclosure where the sensor will be used. The CH_4 concentrations in a naturally ventilated dairy barn change with the positions of gas sampling points and climatic conditions. In one study, the average CH4 concentrations were reported to be 15.1-15.17 ppm at the lowest sampling height from the ground (h = 0.6 m) and 18.75-27.47 ppm at the highest sampling height (h = 2.7 m) for two gas sampling locations in a naturally ventilated dairy barn under the conditions of low wind speeds (less than 3 m/s). The average CH4 concentrations were reported to be 17.38-19.24 ppm at the lowest sampling height from the ground (h = 0.6 m) and 15.52-16.40 ppm at the highest sampling height (h = 2.7 m) for two gas sampling locations in the same dairy barn under the conditions of high wind speeds (more than 3 m/s). A decreasing trend in CH_4 concentrations with increasing sampling height was observed at high wind speeds (Sahu et al., 2023). These results show that the CH_4 concentrations in naturally ventilated farms are around 20 ppm.

Many calibration models have already been proposed in the literature. One of these models is a multi-variable linear regression equation. In this model, sensor response, water vapor concentration and the interaction between sensor response and water vapor was considered (Furuta et al., 2022). Five low-cost, off-shelf MOx sensors (TGS2611-E00, TGS2611-C00, TGS2600, TGS2602 and MQ4) were compared to monitor the methane concentrations at atmospheric levels. The calibration equation for TGS2611-E00 sensors gave best predictions (R^2=0.76-0.78 and RMSE=1.18 and 1.22 ppm). This study showed the water vapor significantly affected the sensor response by both individually and interactively. The authors mentioned that not controlling humidity levels independently of temperature shaded the individual and interactive effect of gas temperature.

Bastviken et al. (2020) calibrated the Figaro NGM26611-E13 module having a TGS2611-E00 sensor. The CH_4 concentrations were changed from 2 to 719 ppm by direct injections of methane into the calibration chamber by syringe via a tube during the calibration experiments. Multiple calibration experiments were performed by changing temperature (T) from 10 to 42 °C and relative humidity from 18% to 70%. They used three different approaches to develop adequate calibration models. In the first approach, they proposed a two-step calibration procedure. In the first step, they tested the effects of temperature and relative humidity on the reference sensor resistance (R_0), the total of the reference resistance (R_L), and resistance caused by atmospheric CH_4 level (R_{Sbkg}). In the second step, they correlated CH_4 mole fractions with R_S/R_0, temperature and relative humidity. In the second approach, they predicted the model parameters in Step 2 from the parameters derived in Step 1. In the third approach, they hypothesized that the calibration data for each sensor were subsampled randomly, and these random subset data were combined with the minimum voltage across the reference resistor (V_L) data to derive calibration parameters as done in Approach I. They reported that Methane Prediction Model (CH_4 Model 5) had the highest prediction performance:

$$\boldsymbol{CH_4} = aR^b + cH(aR^b) + K \tag{9}$$

In this equation, $\mathbf{CH_4}$ is the concentration of methane in ppm; R is the ratio of R_S/R_0; H is absolute humidity, a,b,c and K are model parameters estimated from calibration data.

To calculate R_0, the following equation is used;

$$\frac{R_S}{R_0} = \frac{\left(\frac{V_C}{V_L}-1\right)}{\left(\frac{V_C}{V_0}-1\right)} \tag{10}$$

In this equation V_C is the total circuit voltage(5V), V_L is the voltage across the reference resistor, which given by the sensor. V_0 is the lowest measured sensor output voltage representing atmospheric levels. V_0 is calculated by the following equation:

$$V_0 = gT + S \tag{11}$$

Bastviken et al.(2020) did not give the values of model parameters in Equations 9 and 11. They recommended the users to find this values for each sensor they would use. On the other hand, Ragnoli and Singer (2024) gave the values of these parameters as g=0.02296599, S=0.80312184, a=7.82970298 b=-1.90113967 c=0.02550936 and K=0.53696045. These parameters values were used in this thesis.

Absolute humidity (H) plays a crucial role in methane prediction, as moisture affects sensor readings. It is derived from the measured relative humidity and temperature values of indoor air using method given by Vaisala (2013), which assumes the behavior of an ideal gas.

Water vapor saturation pressure (Pws) is firstly calculated as follows ;

$$Pws = A.10^{\left(\frac{mT}{T+T_n}\right)} \tag{12}$$

Where Pws is the saturation pressure over water (hPa) at temperature T (in °C), and A, m and T_n are constants determined by empirical data for temperatures between -20°C and +50°C

Secondly, Dew Point Pressure (Pw) is calculated as follows;

$$Pw = Pws \times \frac{RH}{100} \tag{13}$$

Where Pw is the dew point (in hpa) and RH is the relative humidity (in %).

Absolute humidity, the mass of water vapour in a certain volume can be calculated assuming ideal gas behaviour.

$$H = \frac{C}{T+273.15} \cdot \frac{Pw}{100} \tag{14}$$

Where H is the absolute humidity (in g m^{-3}) and C is a constant (in gKJ^{-1})

In Equations 12 and 14, A is 6.116461, m is 7.591386, T_n is 240.7263 and C is 2.16679

In a naturally ventilated barn, NH_3 concentration levels tend to increase with sampling height, particularly during low wind speed conditions, where the concentration at the top (2.7 m) was recorded at 3.95–5.00 ppm, 105.1% higher than at the lowest sampling height (0.6 m). Under high wind speeds, NH_3 still exhibited an increasing trend with height but to a lesser extent, with concentrations rising by 10.09 % at 2.7 m compared to the baseline. These findings indicate that NH_3 emissions are affected by turbulent airflow and dilution effects, emphasizing the need for well-positioned sensors to accurately capture ammonia dispersion. The observed trends in NH_3 concentrations underscore the importance of wind speed, sensor placement, and ventilation efficiency in dairy barns, which directly influence gas measurements and environmental impact assessments (Sahu et al., 2023).

To integrate the MQ137 ammonia sensor into the circuit, a load resistance (R_L) is used as a voltage divider. Although various values for R_L is employed, a load resistance of 47 kΩ is recommended. The sensitivity curve of the MQ137 ammonia sensor is logarithmic, showing a relationship between the ratio of the sensor resistance at any given concentration $\frac{R_S}{R_0}$ and the ammonia concentration (ppm). This curve is characterized by a slope (m) of -0.243 and an intercept (b) of 0.323. In clean air, the sensor resistance (R_S) is 30 kΩ, and the $\frac{R_S}{R_0}$ ratio is 3.6 (Raj, 2018). The electric scheme of the MQ137 sensor module is presented on (Figure 13).

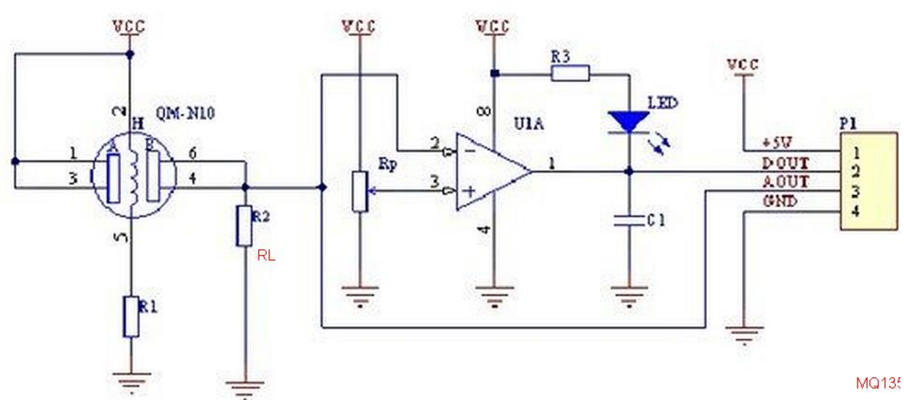

Figure 13: Electric scheme of the MQ137 sensor module

Check on the sensitivity characteristic graph which is plotted against $\frac{R_S}{R_O}$ and PPM. this is the one that we need for our calculations. (Figure 14).

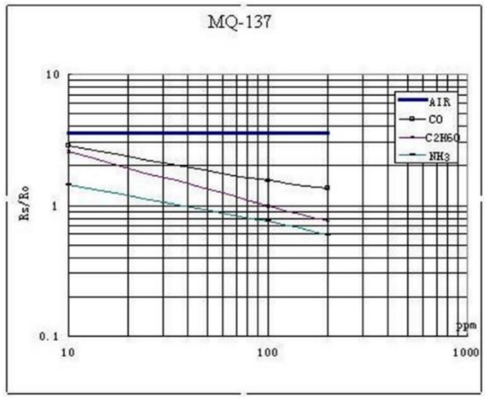

<u>Figure 14</u>: Typical sensitivity characteristics of the MQ-137 for several gases.

Rs is calculated based on the given conditions. The ratio of $\frac{R_S}{R_0}$ is 3.6, as shown in the graph. The supply voltage (Vc) is +5V, and the load resistor (R_L) is 47 kΩ.

$$R_S = (\frac{V_C}{V_{RL}} - 1\ ) \times R_0 \tag{15}$$

The sensor was heated for 24 hours and left in open air. After this period, the 'R_0 in fresh air' value was monitored through the Arduino IDE serial console. The 'R_0' value was then adjusted in the MQ137 program accordingly

It is concluded that the value of R_0 is approximately 95KΩ for the sensor. With the known value of R_0, Rs can be easily calculated using the formulas provided above. The previously calculated value of Rs pertains to fresh air and will differ when ammonia is present; however, calculating Rs is straightforward and is directly determined in the final program. Before running the program, the values for Load resistance (R_L), Slope (m), Intercept (b), and Resistance in fresh air (R_0) must be inputted. (Anonymous, 2017).
The calibration method for the MQ137 sensor relies on factory-provided parameters, which are generalized and may not accurately account for variations in individual sensors. Ideally,

each MQ137 sensor should undergo individual calibration to correct specific errors. The sensor generates analog data, which is first converted to voltage and then to a physical parameter sensor resistance. To establish baseline resistance (Ro), the sensor must be exposed to a zero-ammonia environment for 24 to 48 hours. Once Ro is determined, ammonia concentration is calculated based on the ratio of the sensor's current resistance to Ro.

To convert the analog output of the MQ137 sensor into meaningful data, the output is first converted into a voltage variation:

$$V_{MQ137} = AnalogRead \times \left(\frac{5}{1023}\right) \tag{16}$$

Next, the voltage is used to calculate the sensor resistance (R_S) using the equation :

$$R_S = R_L \times \left(\frac{5}{V_{MQ137}} - 1\right) \tag{17}$$

Where R_L is the load resistance, typically set to 1 kΩ in this case.

To determine the baseline resistance (R_0), the sensor must undergo a conditioning period of two days in an ammonia-free environment. The R_0 value is obtained by continuously monitoring the resistance and averaging the results. Once R_0 is established, the ammonia concentration can be calculated using the ratio provided in the sensor's datasheet.:

$$Concentration = f\left(\frac{R_S}{R_0}\right) \tag{18}$$

This equation defines the relationship between the $\frac{R_S}{R_0}$ ratio and the gas concentration, expressed in parts per million (ppm).

3.2. Manufacturing Of Air Quality Monitoring System

Before beginning the wiring process, it is essential to review the datasheets of all sensors to understand their specifications. Five sensors will be connected to an Arduino Nano. A custom PCB can be used to facilitate the connection of the sensors. The specific function of each sensor is outlined as follows:

The KE 25 sensor oxygen does not require an external power source, as it generates its own voltage. The output voltage ranges from approximately 0 to 70 mV. However, this signal is too weak to be directly read by a microcontroller, such as the Arduino Nano, and therefore requires amplification. To amplify the sensor output, an LM358 operational amplifier (op-amp) IC will be utilized (Anonymous, 2020a).

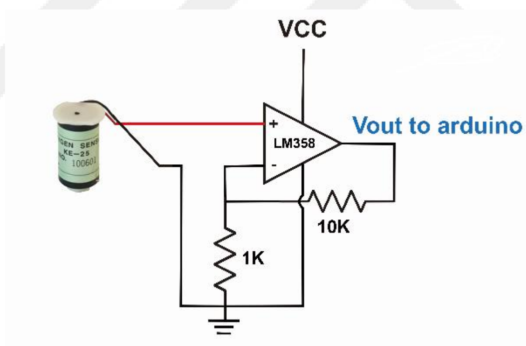

Figure 15: Figaro KE 25 oxygen sensor connection circuit

The amplifier is connected to the PCB along with the Arduino. Using the Arduino IDE, the sensor's output can be read easily through the Analog-to-Digital Converter (ADC). The ADC reads a value of approximately 75 ; to convert this into a standard oxygen concentration of 21% in the air, the ADC value must be multiplied by a factor of 0.28. Calibration of the oxygen concentration is necessary for accurate readings.

The TGS2611 sensor, housed in a standard TO-5 package, is designed to operate with a heating current of 56 mA. Methane concentrations affect the sensor's resistance (R_S). The sensor operates with two voltage inputs: the heater voltage (V_H) and the circuit voltage (V_C), both powered by +5 volts. Pin 1 is connected to +5 volts, and Pin 4 to ground, with similar connections for Pins 3 and 2. A load resistor (R_L) is placed between Pin 2 and ground, and the voltage signal (VR_L) is measured across R_L, which is proportional to the methane concentration detected by the TGS2611. The sensor resistance (R_S), load resistor (R_L), circuit voltage (V_C), and voltage signal (VR_L) are calculated using Equation 1, while power dissipation is determined using Equation 2.

The MH-Z16 sensor is equipped with a UART interface. Using an adapter (I2C to UART bridge IC SC16IS750), the sensor was connected to an I2C interface, thereby conserving two I/O pins. An "auto self-calibration" algorithm is embedded in the sensor's firmware. This algorithm is operated continuously by tracking the sensor's lowest reading. After 24 hours, the lowest value (denoted as value A) is recorded. After 48 hours, the lowest value from the previous 24 hours (denoted as value B) is recorded. The algorithm then compares values A and B, and if they match, the new value is set as the baseline. This process is repeated for subsequent cycles. According to the manufacturer, long-term drift is effectively mitigated by this algorithm, particularly in applications where the sensor is exposed to fresh air at least once every 24 hours. For instance, in environments where CO2 concentration occasionally drops to around 400 ppm (the minimum expected in fresh air), the algorithm functions effectively. However, in environments with consistently low or high CO_2 concentrations, such as greenhouses, challenges may arise. To interrupt or disable the auto-calibration cycle, the sensor must be powered off at least once every 24 hours. This can be achieved by toggling PIN15 of the SC16IS750 via the I2C interface. PIN16 of the SC16IS750 is used as a calibration signal for the sensor, while PIN15 is connected to a power MOSFET to control the sensor's power. Both PIN15 and PIN16 can be controlled through software via the I2C interface (Anonymous, 2013). (Figure 18).

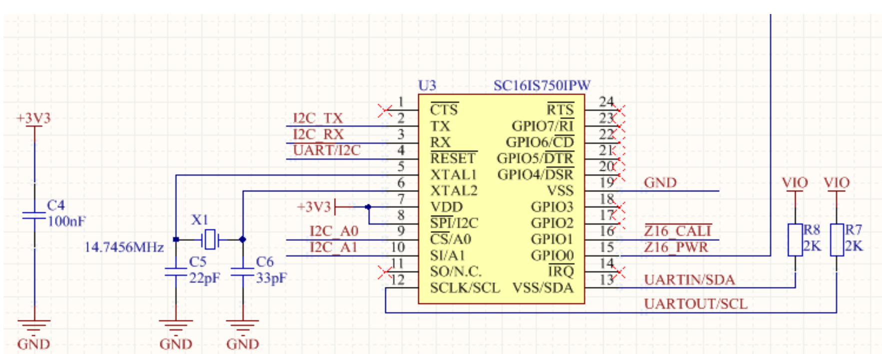

Figure 16: Schematics of the UART – I2C bridge chip

The sensor is equipped with four pins; VCC: Module power supply –2.4V to 5V; GND; SDA: I2C data; SCL: I2C clock with no designated function.

Before using it, the frequency has to be known. It's generally written on the backside of LoRa in library according to the LoRa we will use. In this case it's 433Mhz.

The project requires the design and manufacturing of many different PCB boards, which serve to interconnect components and facilitate communication between them. Utilizing a PCB minimizes wiring errors and enhances overall system stability by providing a compact and organized platform for component integration. By consolidating multiple functions onto a single board, space utilization is optimized, and signal flow is streamlined, ensuring efficient communication between various parts of the system. As an initial step in the development process, the PCB board for the gas measurement unit was designed and implemented. The following sequence of operations was followed in the design and manufacturing of the PCB boards:

1. Sensors and electronic circuit elements were connected to the PCB board.

2. The PCB board circuit was first created on the breadboard (Figure 17).

3. The PCB board circuit was drawn in the circuit design program (Figure 18).

4. The PCB board circuit was printed (Figure 20).

5. Sensors and electronic circuit elements were soldered onto the printed PCB board (Figure 21).

Due to recurring errors in the design and manufacturing of PCB boards, such as short circuits and missing traces, the process was repeated multiple times to ensure accuracy. In this study, all amplifiers and sensors, including the LM358 IC, MQ-137, DHT22, TGS26, NGM2611-C13 (with the module), KE-25, and CMD7162, were integrated into the PCB. The schematic was designed using EASYEDA, with components created through its library system. Most project components were custom-designed, including 3D models for each part to achieve a 3D PCB layout. The final designs were saved as .STEP files for seamless import into other design tools. The PCB was 73mm wide and 64 mm long (Figure 17).

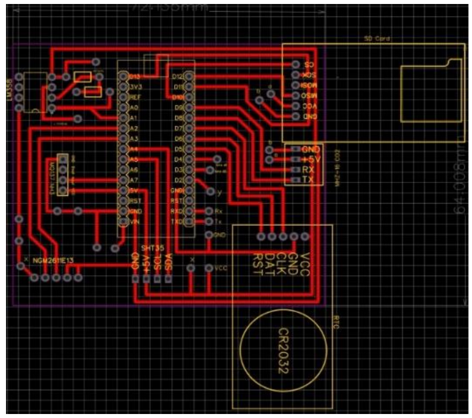

Figure 17: System connection schematic (PCB)

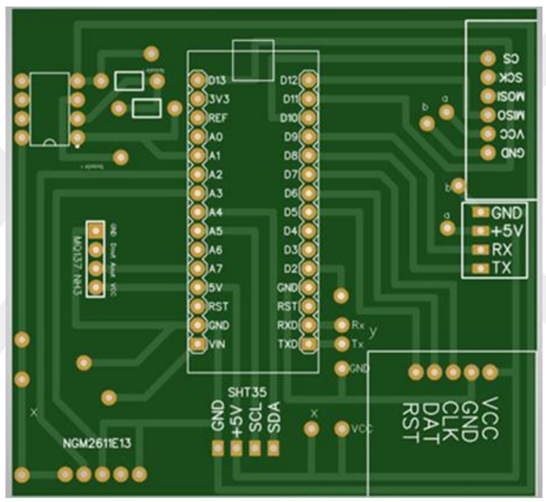

Figure 18 : printed circuit

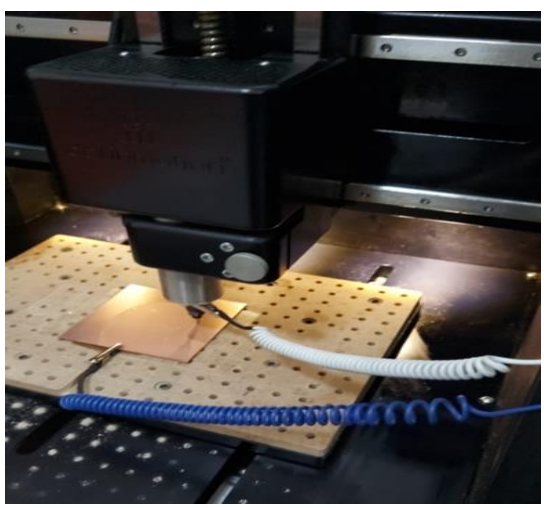

Figure 19: Printing the circuit with CNN routeur

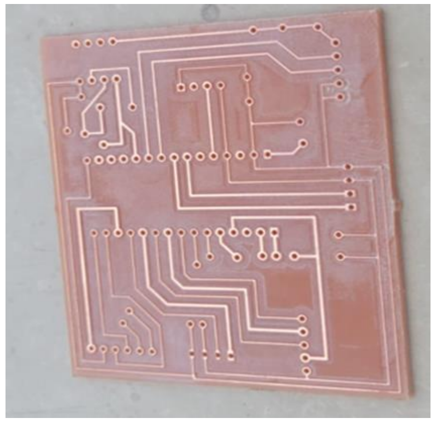

Figure 20: Completed printing circuit

The smallest components were soldered first, followed by the insertion of resistors and transistors. The pin connectors and the ARDUINO NANO board were then soldered, ensuring compatibility with the specific pin layout, as variations may exist. Subsequently, all sensors were positioned in their designated locations. Two capacitors were incorporated into the design to store electrical charges. The power supply for the board was provided through a mini-USB connector, delivering a 5V input. Additionally, two switches were soldered into place. For the DS3231 real-time clock module, the pins were carefully bent before soldering. Once secured, the battery was inserted to maintain timekeeping even in the event of a power loss to the main PCB. Finally, a multimeter was used to verify that the signal reached the appropriate pins on the board, ensuring proper functionality. If the signal does not reach the pins, they can be cleaned with alcohol before proceeding with any programming (Figure 21).

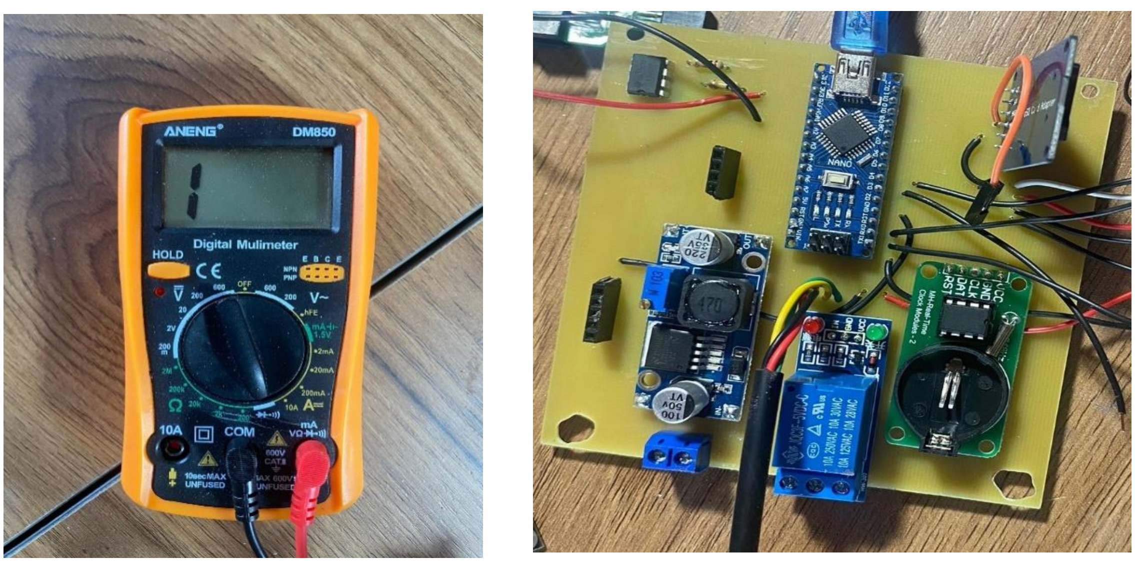

Figure 21: The PCB plate designed for installation with the sensors system plugged in

The PCB was fixed within a large, hermetically sealed casing, which incorporates two fans to facilitate airflow and support the regeneration of condensed air. The case also contains a power supply, a LoRa module, a battery, an electrical circuit breaker, as well as various bolts and nuts for secure assembly. Adequate ventilation was ensured to prevent overheating, as excessive heat could compromise measurement accuracy.

The RMGF DZ47s circuit breaker was integrated with the power supply to protect the system sensors from potential damage caused by overcurrent, short circuits, or overloads. The battery was connected to the output of the power supply, ensuring correct polarity alignment for each terminal. To program the ARDUINO NANO board, a USB connection is established between the serial UART interface and the programming header. Before plugging the USB into the computer, it is essential to turn on the device's main power. This step is critical since the power provided by the computer's USB port, limited to 500mA, may not be adequate for proper operation. The process of uploading a sketch to the ARDUINO NANO involved selecting the appropriate board within the Arduino IDE, choosing the correct version and processor port, and using libraries for each sensor. The Arduino then reads sensor data and transmits it to the computer.

The PCB board of the manufactured gas unit, along with the sensors, is housed within a plastic enclosure. The battery was connected to the power supply output, ensuring correct polarity alignment for each terminal. The air quality monitoring system is powered via a Mini USB connector, which can draw 5 volts from sources such as a 5V USB adapter, a phone charger, or a power bank. Once the device is powered on, the program can be uploaded. To program the ARDUINO NANO board, a USB cable is connected from the serial UART interface to the programming header. Before plugging the USB cable into the computer, it is important to ensure that the device's main power is turned on, as the USB power supply from the computer, which is limited to 500mA, may not provide sufficient current for proper operation. The steps for uploading a sketch to an ARDUINO NANO board included selecting the appropriate board in the Arduino IDE, choosing the correct version and processor port, and using the required libraries for each sensor. The Arduino reads data from the sensors and transmits it to the computer. Initial attempts to read values from the methane and ammonia sensors using the LoRa MQTT protocol resulted in both sensors displaying zero values. Upon investigation, we discovered an issue with the methane sensor system. To resolve this, we modified the OUT and IN pins on the system circuit (PCB). After making these adjustments, the methane sensor began to function correctly, displaying values ranging from 0.5 to 1.16 ppm. The experiment was conducted in three stages: system design and manufacture, installation and data collection, followed by data analysis to assess air quality. A wireless sensor network is used to provide real-time data.

3.3. Air Quality Evaluation

The air quality evaluation system has been developed to monitor and assess environmental conditions that can negatively affect livestock health and productivity. By using predefined threshold values for stress variables, such as harmful gas concentrations (e.g., CO_2, NH_3, CH_4), the system identifies when these levels exceed safe limits. A code can be implemented to promptly inform farmers whenever such exceedances occur, enabling them to take immediate corrective actions. One of the critical objectives of this work is to quantify the duration for which cows are exposed to these harmful gases, providing insights into their potential impact on animal health and welfare. This analysis helps farmers better manage their environment, reduce prolonged exposure to stress factors, and improve overall livestock conditions. The code is provided in Appendix .

a) Stress Variable (SV)

Stress variable can be any physical factor causing animal stress. The undesired high concentrations of CO_2, NH_3, and CH_4 can be stress variables in addition to THI which causes heat stress.

b) Measurement Values (MV)

The measurement value is the value of the stress variable determined by measurement at a given time

c) Individual Stress Load value (ISLV)

Individual stress Load value is the difference between the Measure Value and the Threshold Value (TV) for a stress variable at a given time.

The equation for individual Load values for all stress variables considered in this study can be calculated as follows;

$$ISLV_{CO2} = MV_{CO2} - TV_{CO2} \quad (13a)$$

$$ISLV_{NH3} = MV_{NH3} - TV_{NH3} \quad (13b)$$

$$ISLV_{CH4} = MV_{CH4} - TV_{CH4} \quad (13c)$$

$$ISLV_{THI} = MV_{THI} - TV_{THI} \quad (13d)$$

d) Daily Stress Load value (DSLV)

Daily Stress Load value (DSLV) is the sum of weighed individual load values in a given day.

$$DSLV = \sum_{i=1}^{n} ISLV_i \times \frac{MI}{24} \qquad (14)$$

Where, MI is the measurement interval which has the unit of hour. The constant of 24 represents the number of hours in a day. The daily number of measurements (n) can be calculated as follows ;

$$n = \frac{24}{MI} \qquad (15)$$

For the measurement interval of 10 minutes (0.1667 hours), *n* is equal to 144.

e) Daily Stress Duration (DSD)

If the measurement value is bigger than the threshold value of the selected stress variable, Individual Stress Duration (ISD) is equal to 1. If the measurement value is less than or equal to the threshold value of the selected stress variable, Individual Stress Duration (ISD) is equal to 0. Then, Daily Stress Duration can be calculated as follows;

$$DSD = \sum_{i=1}^{n} ISD_i \times MI \qquad (16)$$

4. RESULTS and DISCUSSION

The air quality monitoring system that was successfully manufactured is presented in Figure 22.

Figure 22: Air quality monitoring system

In this study, an air quality monitoring system with various sensors was designed and implemented using the Arduino electronic platform. This unit monitors indoor air quality factors including temperature, relative humidity, and gas concentrations. The system is based on a reproducible methodology, and the source code used for control and data collection is provided. The sensors are connected to the Arduino electronic platform and calibrated to detect target gases such as methane (CH_4), ammonia (NH_3), and carbon dioxide (CO_2). The source code collects analog signals from the sensors and converts them to digital concentrations. The data are compared to reference values to assess the effectiveness of the calibration. The Arduino code used is given in Appendix. The indoor air is forced to flow through the inside of the air quality monitoring system by a fan to have accurate sensor readings. The system operates on battery power. The PCB board integrates sensors to measure ammonia concentration (ppm), methane concentration (ppm), carbon dioxide concentration (ppm), and oxygen concentration (ppm), relative humidity (%), and temperature (°C). Gas concentrations were recorded successfully after adjustments to the PCB circuitry. The design focuses on real-time monitoring based on the wireless communication having a LoRa module. for data collection.

The air quality monitoring system was placed on a dairy barn to collect some indoor data (Figure 23). The data collected from the dairy barn are given in Table 2.

Figure 23: Overview of the air quality monitoring system installed in a dairy barn

Table 2: Measured values of gas concentrations and climatic parameters

Date	Time	Ammonia	Methane	Temperature	Relative Humidity	Oxygen	Carbone Dioxide
2024-09-21	14 :49	0.00	15	27.16	36.49	227.640	417
	14 :50	0.00	16	27.20	35.87	240.240	392
	15 :23	0.02	19	27.36	38.18	217.280	503
	15 :34	0.01	23	27.97	37.11	242.480	499
	15 :56	0.00	18	27.76	36.11	234.360	429
	16 :18	0.00	23	27.84	35.87	235.480	425
	16 :29	0.00	19	27.88	37.92	243.880	490
	16 :52	0.00	13	27.63	37.67	235.760	411
2024-10-18	14 :07	0.05	13	18.44	39	239.680	515
	14 :12	0.03	14	18.25	39.45	217.840	457
	14 :44	0.02	15	18.37	40.44	220.920	521
	14 :59	0.19	15	18.41	39.86	219.240	526
	15 :15	0.06	18	18.44	40.10	214.480	546
2024-11-03	09 :10	0.21	18	18.63	39.15	235.200	530

The measured values ranged from 0.00 to 0.21 ppm for ammonia and 13 to 23 ppm for methane from 392 to 546 for carbon dioxide, from 214.480 to 243.880 for oxygen, from 18.25°C to 27.97°C for temperature and from 35.87% to 40.44% for relative humidity. The ammonia concentrations are much lower than the values reported in the literature. Therefore, the ammonia sensor (MQ137) needs further calibration. On the other hand, the methane sensor (TGS2611-E00), the carbon dioxide sensor (MHZ16), the oxygen sensor (KE-25), and the temperature/relative humidity sensor (SHT 35) gave acceptable results. The use of off-the-shelf sensors and components makes the system affordable for farm-scale implementation. Wireless data transmission using LoRa enables timely responses to air quality changes. The system design supports easy updates and troubleshooting.

Table 3 gives the threshold values for NH_3, CH_4, and CO_2 recommended for different livestock species. These values serve as benchmarks to ensure animal comfort and health (Yıldırım and Açar, 2023). The threshold values change based on animal species as seen in Table 3.

Table 3: Recommended thresholds for gas concentrations according to animal species

Gases	Cattle	Horse	Poultry	Sheep	pigs
NH_3	<10 ppm	<10 ppm	<20 ppm	<60 ppm	10-20
CH_4	<10.000 ppm	<10.000 ppm	1000-5000 ppm	<10.000	<10.000
H_2S	<0.5 ppm <0.016%	<0.016%	<0.008 %	<0.016	<0.016
CO_2	<2000 ppm <3000 ppm	<3000 ppm	5000-30.000 ppm <1000 ppm	<3000 ppm	5000-30.000 ppm <10.000
CO	<50 ppm	<50 ppm	<50 ppm	<50 ppm < 50 ppm	<50 ppm

The ammonia (NH_3) concentration must be below 10 ppm for cattle In this study, the measured ammonia levels were exceptionally low, with a maximum value of 0.21 ppm. These concentrations are well within the acceptable limits, indicating excellent air quality with respect to NH_3 exposure.

For methane (CH_4), the permissible concentration for most livestock species is below 10,000 ppm. The CH_4 concentrations observed in this study ranged between 0.13 and 0.23 ppm, which is significantly lower than the established threshold. These findings suggest minimal methane emissions within the monitored environment.

The recommended carbon dioxide (CO_2) concentrations vary by species, with thresholds generally below 2,000 ppm for cattle and up to 10,000 ppm for poultry and sheep. The measured CO_2 levels ranged from 392 to 546 ppm, remaining well below all critical thresholds. This indicates that carbon dioxide concentrations are within safe and acceptable limits. Oxygen levels were measured between 214.48 and 243.88 ppm.

Temperature-Humidity Index (THI) values were calculated by using Equation 1 to assess the combined impact of heat and moisture on animal well-being. THI values across all intervals ranged from 69.78 to 72.14, with only one instance exceeding the threshold of 72, which is typically associated with heat stress. The total duration of stress recorded was minimal, lasting just 10 minutes.

The concentrations of ammonia, methane and carbon dioxide stayed significantly below their threshold values. These results showed that animal well-being was provided. Even though the extreme indoor air quality conditions were not observed during the trial period, key metrics including Individual Stress Load Value (ISLV), and Daily Stress Duration (DSD) were calculated. THI values were given in Table 4 for the selected three cases. In Case 1, the THI value exceeded the threshold, indicating heat stress. THI values remained below the threshold value of THI in Cases 2 and 3, showing that there is no heat stress. (Table 4). All cases recorded low NH_3 levels, with no exceedance of the threshold. There wasn't any ammonia-related stress that was detected. (Table 5). CH_4 levels in all cases were below the threshold. There wasn't methane-related stress that was identified (Table 6). CO_2 values ranged from 417 to 530 ppm, all below the stress threshold. there was no stress was observed due to CO_2 exposure. (Table7).

Table 4: THI values with Daily Stress Duration

CASE	Temperature	Relative humidity	THI	Exceeds Threshold	DSD
1	26.6	36.81	75.54	Yes	Calculated
2	18.38	39.77	66.37	No	0
3	18.63	39.15	62.66	No	0

Table 5: Ammonia values with Daily Stress Duration

CASE	Ammonia	Exceeds Threshold	DSD
1	0.00	NO	0
2	0.19	NO	0
3	0.21	NO	0

Table 6: Methane values with Daily Stress Duration

CASE	METHANE	Exceed Threshold	DSD
1	0.18	NO	0
2	0.18	NO	0
3	0.23	NO	0

Table 7: Carbone Dioxide values with Daily Stress Duration

CASE	Carbone Dioxide	Exceed Threshold	DSD
1	417	NO	0
2	521	NO	0
3	530	NO	0

These findings confirm that gas concentrations are well within acceptable levels, indicating no risk of gas-related stress in the environment. Ammonia levels were compared to a threshold of 25 ppm, above which health risks to humans and animals become a concern. Throughout the day, ammonia levels were extremely low, ranging from 0.00 ppm to 0.02 ppm. There were no instances where ammonia concentrations approached or exceeded the threshold, resulting in zero minutes of daily stress duration. These negligible ammonia levels reflect excellent air quality regarding ammonia levels. Carbon dioxide concentrations were assessed relative to a threshold of 2000 ppm, a level associated with poor air quality and potential health risks. Measured CO_2 levels ranged from 392 ppm to 503 ppm, remaining well below the threshold. No intervals recorded CO_2 concentrations above the safe limit, resulting in zero minutes of daily stress duration. The CO_2 levels indicate a well-ventilated environment, with concentrations consistent with typical atmospheric conditions. The data illustrates an environment largely free from harmful stressors. Except for a brief period of heat stress indicated by the THI values, all other parameters—methane, ammonia, and carbon dioxide—remained well below their respective thresholds. This suggests the environment is well-managed and conducive to maintaining good air quality and comfort. Its current performance meets basic requirements but highlights the trade-offs between affordability and precision. Addressing these weaknesses through targeted improvements will significantly enhance its reliability and usability.

The thesis stands out by highlighting several points of originality, including the design of a multiple sensor unit that can be available to many animal farms; the use of calibration techniques by inserting values into equations adapted to the different sensors to guarantee precise measurements in varied environments and Evaluating Threshold Values by Implementing a Code to Alert Farmers When THI Exceeds Safe Levels.

The development of an available multi-sensor unit designed specifically for many dairy farms marks a notable advancement in barn air quality monitoring. The system prioritizes affordability by utilizing available materials and efficient manufacturing methods. Custom-designed printed circuit boards (PCBs) were employed to improve sensor arrangement while reducing production expenses. By providing a cost-effective yet efficient system, this research seeks to enable big and medium-scale farms to maintain ideal environmental conditions, improving livestock health and productivity while reducing their environmental impact.

5. CONCLUSION and SUGGESTIONS

The system consists of sensors for which gases are most harmful in barns. The selection of sensors was made based on several criteria such as measurement capability in harsh conditions, concentration range, internet connectivity, and ease of access to measured data. The work carried out will be a boon for farmers to improve the comfort of farm animals. The factors that generally affect gas and dust production in livestock facilities are the climatic environment, animals, building and manure management.

The thesis highlights the development of an air quality monitoring system on farms, highlighting the crucial importance of data collection to reduce harmful gas concentrations. In a context where agriculture is often singled out for its role in environmental degradation, this innovative system aims to provide concrete and effective solutions. The experimental results obtained during this research demonstrate that this system can provide real-time monitoring of air quality, thus enabling early detection of pollutants and variations in atmospheric composition. With the help of sensing sensors and advanced analysis algorithms, farmers can continuously monitor levels of carbon dioxide, methane and other harmful gases, facilitating proactive management of emissions.

By improving air quality on farms, this system not only contributes to the health and well-being of animals, which are sensitive to environmental changes, but also plays a key role in mitigating the environmental impact of livestock farming. Indeed, better air quality can reduce stress in animals, which translates into improved productivity and overall health.

In addition, collecting accurate and real-time data allows farmers to make informed decisions about their livestock and resource management practices. For example, they can adjust livestock conditions, optimize animal feeding or implement emission reduction strategies, contributing to more sustainable and environmentally friendly livestock farming.

In summary, this thesis highlights the importance of integrating advanced monitoring technologies into barn environments, not only to address current environmental challenges but also to promote sustainable practices that prioritize animal welfare and the health of our planet.

REFERENCES

Anonymous, 2010. What is SOLIDWORKS file format and how to open it? https://cadexchanger.com/solidworks/?utm

Anonymous, (2013a). Code of Practice for the Care and Handling of Sheep. https://www.nfacc.ca/sheep-code

Anonymous, (2013b). MH-Z16 NDIR CO_2 Sensor with I2C/UART Interface Board MH-Z16 NDIR CO2 Sensor with I2C/UART Interface Board | Sandbox Electronics

Anonymous, (2015). Ammonia Gas Sensor Model：MQ137 https://www.winsen-sensor.com/d/files/semiconductor/mq137.pdf?utm

Anonymous, 2016. DHT11 & DHT22 Sensors Temperature and Humidity Tutorial using Arduino https://howtomechatronics.com/tutorials/arduino/dht11-dht22-sensors-temperature-and-humidity-tutorial-using-arduino/ (23/05/2024)

Anonymous, 2017. Arduino MQ137 PPM Sensor https://www.instructables.com/MQ137-PPM-Sensor/ (15/02/2024)

Anonymous, 2018a. Temperature and humidity monitoring with Arduino-DHT22 https://www.arducoding.com/2018/05/arduino-temperature-and-humadity.html

Anonymous, 2018b. Introduction to Arduino IDE https://www.theengineeringprojects.com/2018/10/introduction-to-arduino-ide.html(08.03.2024)

Anonymous, 2020a. How to use KE-25 oxygen sensor https://www.youtube.com/watch?v=-ZsXkOzD0Uk (31/12/2023)

Anonymous, 2020b. Arduino humidity sensors: testing and calibration https://www.bing.com/videos/riverview/relatedvideo?&q=Calibration+DHT22+ASTM+&&mid=2A89F8779D34F4FDA30A2A89F8779D34F4FDA30A&&FORM=VRDGAR

Anonymous, 2020c. Sensor Fundamentals Data Acquisition Basics and Terminology https://www.youtube.com/watch?v=Xc8dP0PdC_(02/02/2024)

Anonymous, 2021a. How to use sensors with Arduino https://www.youtube.com/watch?v=q9UCSynDEw8 (10/02/2024)

Anonymous, 2021b. Introduction to ESP32 - Getting Started https://www.youtube.com/watch?v=xPlN_Tk3VLQ (03.10.2023)

Anonymous, 2023. ESP32 ADC – Read Analog Values with Arduino IDE https://randomnerdtutorials.com/esp32-adc-analog-read-arduino-ide/

Anonymous, 2024a. Heat stress: what is it and how is it measured? https://climate.copernicus.eu/heat-stress-what-it-and-how-it-measured

Anonymous, 2024b. LoRa https://en.wikipedia.org/wiki/LoRa

Anonymous, 2024c. Send Receive SMS & Call with SIM800L GSM Module & Arduino In-Depth: Send Receive SMS & Call with SIM800L GSM Module & Arduino (lastminuteengineers.com) (20/04/2024)

Anonymous, 2024d. Fritzing https://en.wikipedia.org/wiki/Fritzing#:~:text=Fritzing%20is%20an%20open-source%20initiative%20to%20develop%20amateur,at%20the%20University%20of%20Applied%20Sciences%20Potsdam.%20 (08.03.2024)

Adi, P. D. P., and Kitagawa, A. (2019). Performance evaluation of E32 long range radio

frequency 915 MHz based on internet of things and micro sensors data. International Journal of Advanced Computer Science and Applications, 10(11).
Antunes, A. M. S., 2019. Development of an ammonia portable low-cost air quality station, Doctoral dissertation, university of Lisbon/Portugal, Faculty of Sciences.
Albert J. Heber heber@purdue.edu , Ji-Qin Ni , Teng T. Lim , Pei-Chun Tao , Amy M.Schmidt , Jacek A.Koziel , David B. Beasley , Steven J. Hoff , Richard E. Nicolai , Larry D. Jacobson and Yuanhui Zhang, 2006. Quality Assured Measurements of Animal Building Emissions: Gas Concentrations, Journal of the Air and Waste Management Association, 56:10, 1472-1483, DOI: 10.1080/10473289.2006.10465680
Bačėninaitė, D., Džermeikaitė, K., & Antanaitis, R. (2022). Global warming and dairy cattle: How to control and reduce methane emission. Animals, 12(19), 2687.
Bastviken, D., & Duc, N. T., 2020. Facilitating the use of low-cost methane (CH_4) sensors in flux chambers: calibration, data processing, and describing an open source make-it yourself logger–Arduino code, Linköping University. Biogeosciences, 17(13), 3527 3542.
Bastviken, D., & Varner, R.K., 2020. Technical note: Greenhouse gas flux studies: an automated online system for gas emission measurements in aquatic environments. Hydrology and Earth System Sciences, 24, 3417-3430.)
Biagi, R., Ferrari, M., Venturi, S., Sacco, M., Montegrossi, G., and Tassi, F., 2024. Development and machine learning-based calibration of low-cost multiparametric stations for the measurement of CO_2 and CH_4 in air. Heliyon, 10
Bist, R. B., Subedi, S., Chai, L., & Yang, X. (2023). Ammonia emissions, impacts, and mitigation strategies for poultry production: A critical review. Journal of Environmental Management, 328, 116919.
Bossche, M.V., Rose, N.T., & Wekker, S.F. (2017). Potential of a low-cost gas sensor for atmospheric methane monitoring. Sensors and Actuators B-chemical, 238, 501-509.
Broucek, J. (2014). Production of methane emissions from ruminant husbandry: a review. Journal of Environmental Protection, 5(15), 1482.
Chai, L., Ni, J., Chen, Y., Diehl, C.A., Heber, A.J., & Lim, T.T. (2010). Assessment of Long-Term Gas Sampling Design at Two Commercial Manure-Belt Layer Barns. Journal of the Air & Waste Management Association, 60, 702 - 710.
Chen, C. S., & Chen, W. C. (2019). Research and development of automatic monitoring system for livestock farms. Applied Sciences, 9(6), 1132.
Dalvai Ragnoli, M., & Singer, G. (2024). The River Runner: A low-cost sensor prototype for continuous dissolved greenhouse gas measurements. Journal of Sensors and Sensor Systems, 13, 41–61. https://doi.org/10.5194/jsss-13-41-
Dikmen, S. E. R. D. A. L., & Hansen, P. J. ,2009. Is the temperature-humidity index the best indicator of heat stress in lactating dairy cows in a subtropical environment?. Journal of dairy science, 92(1), 109-116.
Domènech-Gil, G., Duc, N.T., Wikner, J.J., Eriksson, J., Påledal, S.N., Puglisi, D., & Bastviken, D. (2023). Electronic Nose for Improved Environmental Methane Monitoring. Environmental Science & Technology, 58, 352 - 361.
Dong, H., Kang, G., Zhu, Z., Tao, X., Chen, Y., Xin, H., & Harmon, J.D. (2009). Ammonia, Methane, and Carbon Dioxide Concentrations and Emissions of a Hoop Grower-Finisher Swine Barn. Transactions of the ASABE, 52, 1741-1747
EPA. (2004). National Emission Inventory -Ammonia Emissions from Animal Husbandry.

https://www3.epa.gov/ttnchie1/ap42/ch09/related/nh3inventoryfactsheet_jan2004.pdf
Eugster, W., Laundre, J., Eugster, J., & Kling, G.W. (2020). Long-term reliability of the Figaro TGS 2600 solid-state methane sensor under low-Arctic conditions at Toolik Lake, Alaska. Atmospheric Measurement Techniques, 13, 2681-2695.
Eugster, W., & Kling, G. W., 2012. Performance of a low-cost methane sensor for ambient concentration measurements in preliminary studies. Atmospheric Measurement Techniques Discussions, 5(2), 2567-2590.
Eugster, W., Laundre, J., Eugster, J., & Kling, G.W., 2020. Long-term reliability of the Figaro TGS 2600 solid-state methane sensor under low-Arctic conditions at Toolik Lake, Alaska. Atmospheric Measurement Techniques*, 13*, 2681-2695.
FAO and GDP. (2018). Climate change and the global dairy cattle sector – The role of the dairy sector in a low-carbonfuture. Rome. 36 pp. Licence: CC BY-NC-SA- 3.0 IGO
FAO (2010). Dairy production and global climate change – New FAO report assesses dairy greenhouse gas emissions. https://www.fao.org/newsroom/detail/New-FAO-report-assesses-dairy-greenhouse-gas emissions/en#:~:text=Methane%20contributes%20most%20to%20the,38%20percent%20in%20developing%20countries (30/12/2024).
Feng, J., Megerian, S., and Potkonjak, M. (2023). "Model-based calibration for sensor networks," SENSORS, 2003 IEEE,Toronto, ON, Canada, 2003, pp. 737-742 Vol.2,doi: 10.1109/ICSENS.2003.1279039.
Figaro (2013). Product Information. TGS 2611 - for the detection of Methane. https://www.figarosensor.com/product/docs/TGS%202611C00(1013).pdf, Rev:10/13. (10.01.2024).
Figaro (2022). Product Information. NGM2611-E13 - Pre-calibrated Module for Methane. https://www.figarosensor.com/product/docs/TGS%202611C00(1013).pdf, Rev:10/22. (10.01.2024).
Furuta, D., Sayahi, T., Li, J., Wilson, B., Presto, A. & Li, J., (2022). Characterization of inexpensive metal oxide sensor performance for trace methane detection. Atmospheric Measurement Techniques. 15. 5117-5128. 10.5194/amt-15-5117-2022.
Furst, L.C., Feliciano, M., Frare, L.M., & Igrejas, G. (2021). A Portable Device for Methane Measurement Using a Low-Cost Semiconductor Sensor: Development, Calibration and Environmental Applications. Sensors (Basel, Switzerland), 21.)
Glennon, C.R., McQuitty, J.B., Clark, P.C., & Feddes, J.J.(1989). Air quality in pullet barns.) Hari K. K., Nandeesh K. K., Sunny D. V., Sudha E. M., Suseela V., A systematic literature review on prototyping with Arduino: Applications, challenges, advantages, and limitations, Computer Science Review, Volume 40, 2021, 100364, ISSN 1574-0137,
Heber, A. J., Ni, J. Q., Lim, T. T., Tao, P. C., Schmidt, A. M., Koziel, J. A., ... & Zhang, Y. (2006). Quality assured measurements of animal building emissions: Gas concentrations. Journal of the Air & Waste Management Association, 56(10), 1472-1483.
Herbut, P., & Angrecka, S. (2014). Ammonia concentrations in a free-stall dairy barn. Honeycutt, W.T., Ley, M., & Materer, N.F. (2019). Precision and Limits of Detection for Selected Commercially Available, Low-Cost Carbon Dioxide and Methane Gas Sensors. Sensors (Basel, Switzerland), 19.
Janke, D., Bornwin, M., Coorevits, K., Hempel, S., van Overbeke, P., Demeyer, P., Rawat, A., Declerck, A., Amon, T., & Amon, B. (2023). A Low-Cost Wireless Sensor

Network for Barn Climate and Emission Monitoring— Intermediate Results. Atmosphere.
Ji, B., Banhazi, T.M., Perano, K.M., Ghahramani, A., Bowtell, L., Wang, C., & Li, B. (2020). A review of measuring, assessing and mitigating heat stress in dairy cattle. Biosystems Engineering, 199, 4-26.
Kilic, I., Simsek, E., Yaslioglu, E. et al. Air quality measurements in four sheep barns part II: pollutant gas emissions. Environ Sci Pollut Res 28, 19064–19078 (2021).
Kumar, S., and Jasuja, A. 2017. Air quality monitoring system based on IoT using Raspberry Pi, International Conference on Computing, Communication and Automation (ICCCA), Greater Noida, India, 2017, pp. 1341-1346, doi: 10.1109/CCAA.2017.8230005.
Koestoer, R.A., Pancasaputra, N., Roihan, I., & Harinaldi (2019). A simple calibration methods of relative humidity sensor DHT22 for tropical climates based on Arduino data acquisition system.
Laurent S., Michel G., Maria G. V., Manuel A., Fausto B., Field calibration of cluster of low-cost available sensors for air quality monitoring. Part A : Ozone and nitrogen dioxide, Sensors and Actuators B : Chemical, Volume 215, 2015, Pages 249-257, ISSN 0925-4005.

Lovarelli, D., Finzi, A., Mattachini, G., & Riva, E. (2020). A Survey of Dairy Cattle Behavior in Different Barns in Northern Italy. Animals: An Open Access Journal from MDPI,10
Lutsko, N. J. (2021). The Relative Contributions of Temperature and Moisture to Heat Stress Changes under Warming. Journal of Climate, 34(3), 901-917. https://doi.org/10.1175/JCLI-D-20-0262.1
Ma, W., Ji, X., Ding, L., Yang, S. X., Guo, K., & Li, Q. (2024). Automatic Monitoring Methods for Greenhouse and Hazardous Gases Emitted from Ruminant Production Systems: A Review. Sensors, 24(13), 4423.
Mitchell, H.L.; Cox, S.J.; Lewis, H.G. Calibration of a Low-Cost Methane Sensor Using Machine Learning. Sensors 2024, 24, 1066.
Mostert, P. (2018). The impact of diseases in dairy cows on greenhouse gas emissions and economic performance. [internal PhD, WU, Wageningen University]. Wageningen University. https://doi.org/10.18174/445487
Nagahage, E. A. A. D., Nagahage, I. S. P., & Fujino, T. (2019). Calibration and validation of a low-cost capacitive moisture sensor to integrate the automated soil moisture monitoring system. Agriculture, 9(7), 141.
Nardone, A., Ronchi, B., Lacetera, N., Ranieri, M. S., & Bernabucci, U. (2010). Effects of climate changes on animal production and sustainability of livestock systems. Livestock Science, 130(1-3), 57-69.
Peterson, C. B., and Mitloehner, F. M. (2021). Sustainability of the dairy industry: Emissions and mitigation opportunities. Frontiers in Animal Science, 2, 760310.
Petric, M., Dodigović, F., Grčić, I., Markužić, P., Radetić, L., & Topić, M. (2019). Ammonia concentration monitoring using arduino platform. Environmental Engineering-Inženjerstvo okoliša, 6(1), 21-26.
Riddick, S. N., Mauzerall, D. L., Celia, M., Allen, G., Pitt, J., Kang, M., & Riddick, J. C., 2020. The calibration and deployment of a low-cost methane sensor. Atmospheric Environment, 230, 117440.

Riche, E., Baldé, H., Kallil, S., Ouellet, V., Charbonneau, E., Coates, T., Wright, T.,Luimes, P. & Gordon, R. (2023). Comparing thermal conditions inside and outside lactating dairy cattle barns in Canada. Journal of Dairy Science. 106. 10.3168/jds.2022-22870.

Sahu, H., Hempel, S., Amon, T., Zentek, J., Römer, A., & Janke, D. (2023). Concentration Gradients of Ammonia, Methane, and Carbon Dioxide at the Outlet of a Naturally Ventilated Dairy Building. Atmosphere.

Slamet W., Miftakhul M., and Bahri Joni A., 2019. Implementasion Of Calibration in Gas Hazardous Carbon Monoxide, Carbon Dioxide and Methana In Closed Room Using Fuzzy Method, Journal of Physics: Conference Series, Volume 1167, 012063.

Sonwani, S., Shukla, A., 2022. Introduction to Airborne Particulate Matter: Source, Chemistry and Health. (eds) Airborne Particulate Matter. Springer, Singapore. https://doi.org/10.1007/978-981-16-5387-2_1

Stéphane, B., Bassompierre, C., Christelle, G., Suzanne, L., Alain Y. B., 2009. Calibration methods for inertial and magnetic sensors, Sensors and Actuators A: Physical Volume 156, Issue 2, Pages 302-311.

St-Pierre, N. R., Cobanov, B., & Schnitkey, G. (2003). Economic losses from heat stress by US livestock industries. Journal of dairy science, 86, E52-E77.

Sugriwan, I., & Soesanto, O., 2017. Development of TGS2611 methane sensor and SHT11 humidity and temperature sensor for measuring greenhouse gas on peatlands in South Kalimantan, Indonesia. In Journal of Physics: Conference Series (Vol. 853, No. 1, p. 012006). IOP Publishing.Thanh Duc, N., Silverstein, S., Wik, M., Crill, P.M.,

Ucgun, H., Gombeci, F., Yuzgec, U., Yalcin, N., 2020. Real-Time Indoor Air Quality Monitoring System with IoT Based Platform. Bilecik Seyh Edebali University Journal of Science, 7(1), 370-381. https://doi.org/10.35193/bseufbd.730919.

Van Leenen K., Jouret, J., Demeyer, P., Van Driessche, L ., De Cremer, L., Masmeijer, C.,Boyen, F., deprez, P. & Pardon, B., 2020. Associations of barn air quality paramters with ultrasonogrpahic lung lesions, airway inflammation and infection in group-housed calves. Preventive Veterinary Medicine. 181. 105056. 10.1016/j.prevetmed.2020.105056.

Van den Bossche, M., Rose, N. T., & De Wekker, S. F. J., 2017. Potential of a low-cost gas sensor for atmospheric methane monitoring. Sensors and Actuators B: Che VanderZaag, A.,
Riche, E., Baldé, H., Kallil, S., Ouellet, V., Charbonneau, E., Coates, T., Wright, T.,Luimes, P. & Gordon, R. (2023). Comparing thermal conditions inside and outside lactating dairy cattle barns in Canada. Journal of Dairy Science. 106. 10.3168/jds.2022-22870.
Wang, X., Ndegwa, P.M., Joo, H., Neerackal, G.M., Harrison, J.H., Stöckle, C.O., & Liu, H. (2016). Reliable low-cost devices for monitoring ammonia concentrations and emissions in naturally ventilated dairy barns. Environmental pollution, 208 Pt B, 571- 9).

Wikipedia, (2024). Ammonia pollution. https://en.wikipedia.org/wiki/Ammonia_pollution#cite_note-CsutC-4 (30.12.2024).

Wu, C., Yang, F., Brancher, M., Liu, J., Qu, C., Piringer, M., & Schauberger, G. (2020). Determination of ammonia and hydrogen sulfide emissions from a commercial dairy farm with an exercise yard and the health-related impact for residents. Environmental Science and Pollution Research, 27, 37684-37698.

Xiang W., Pius M. N., HungSoo J., George M. N., Joseph H. H., Claudio O. S.,Heping L., Reliable low-cost devices for monitoring ammonia concentrations and emissions in naturally ventilated dairy barns, Environmental Pollution, Volume 208, Part B, 2016, Pages 571-579, ISSN/0269-7491,/.

Yıldırım, F., and Açar, Y. (2023) Evaluation Of Gases Affecting Air Quality in Animal Shelters.New Frontiers in Health Sciences, Eds:O. Oral, K.A. Nalcı. Duvar Yayınları, İzmir, Türkiye,19-44.

YK

APPENDIX

ARDUINO CODES

SHT3x-DIS

```
#include <Arduino.h>
#include <Wire.h>
#include "Adafruit_SHT31.h"
Adafruit_SHT31 sht31 = Adafruit_SHT31();
void setup() {
Serial.begin(9600);
if (! sht31.begin(0x44)) {   // Set to 0x45 for alternate I2C address
Serial.println("Couldn't find SHT31");
while (1) delay(1); }
}void loop() {
float t = sht31.readTemperature();
float h = sht31.readHumidity();
if (! isnan(t)) {  // check if 'is not a number'
Serial.print("Temp *C = "); Serial.print(t); Serial.print("\t\t");
} else {
Serial.println("Failed to read temperature");
}
if (! isnan(h)) {  // check if 'is not a number'
Serial.print("Hum. % = "); Serial.println(h);
} else {
Serial.println("Failed to read humidity"); }
delay(1000);}
```

https://microcontrollerslab.com/sht31-temperature-humidity-sensor-arduino/

```
//////////////////////////////////////////////////////////////////////////////////////////////////////////////////////////////////////////////////////////
```

MQ137

```
/*
```

```
Program to measure gas in ppm using MQ-137 sensor ammonia
program by: SEM GNEPA
*/
#define MQ_sensor A0 //Sensor is connected to A0
void setup() {
Serial.begin(115200);
Serial.println("NH3 in PPM"); //Display a intro message
Serial.println("-ALC-"); //Display a intro message
delay(2000); //Wait for display to show info
}  void loop() {
float VRL= 0.0; // Voltage drop across the MQ sensor
float Rs= 0.0; //Sensor resistance at gas concentration
float ratio=0.0; //Define variable for ratio
float RL = 47; // The value of resistor RL is 47K
float m=-0.243; //Enter calculated Slope
float b= 0.42; //Enter calculated intercept
float Ro= 103.83; //Enter found Ro value
unsigned int analog_value=0;
for(int test_cycle = 1; test_cycle <= 500 ; test_cycle++) //Read the analog output of the sensor for 200 times
{analog_value = analog_value + analogRead(MQ_sensor); //add the values for 200
delay(3);  }
float analog = float (analog_value)/500.0; //Take average
VRL = analog*(5.0/1023.0); //Convert analog value to voltage
Rs = ((5.0 * RL)/ VRL) - RL; //Use formula to get Rs value
ratio = Rs/Ro; //find ratio Rs/Ro
float ppm = pow(10,((log10(ratio) - b) / m)); //Use formula to calculate ppm
Serial.print("NH3 (ppm) = "); //Display a ammonia in ppm
Serial.println(ppm);
Serial.print("Voltage = "); //Display a intro message
```

```
Serial.println(VRL);
delay(2000);}
```

```
//////////////////////////////////////////////////////////////////////////////////////////////////////////////////////////////////////////////////////
```

Oxygen sensor KE-25

```
void setup()
{ Serial.begin(9600);}
void loop()
{  int sensorValue = analogRead(A0);
// print out the value you read:
Serial.print("ADC : ");
Serial.println(sensorValue);
float oksigen = sensorValue * 0.28;
Serial.print(oksigen);
Serial.println("%");
delay(300);}
```

```
//////////////////////////////////////////////////////////////////////////////////////////////////////////////////////////////////////////////////////
```

MH 440 D NDIR

```
#include "MHSensor.h"
MHSensor::MHSensor(int pin,
int adcBitResolution,
float voltageResolution,
float minMeasuring,
float maxMeasuring,
bool debug)
{this->_pin = pin;
this->_voltResolution = voltageResolution;
this->_adcBitResolution = adcBitResolution;
```

```
this->_minMeasuring = minMeasuring;
this->_maxMeasuring = maxMeasuring;
this->_debug = debug;
}void MHSensor::init()
{   pinMode(_pin, INPUT);
}uint16_t MHSensor::getAnalogRead()
{   _adc = analogRead(this->_pin);
return (uint16_t)_adc;
}float MHSensor::getVoltage()
{uint16_t adc = this->getAnalogRead();
_sensorVolt = (adc * _voltResolution) / (pow(2, _adcBitResolution) - 1);
return _sensorVolt;
}float MHSensor::readFromAnalog()
{float volt = this->getVoltage();
if (volt < MIN_OUTPUT_SIGNAL)
return 0.0f;
float ppm = this->mapOutputVoltage(volt, MIN_OUTPUT_SIGNAL, MAX_OUTPUT_SIGNAL, this->_minMeasuring, this->_maxMeasuring);
return ppm;
}float MHSensor::mapOutputVoltage(float val, float inMin, float inMax, float outMin, float outMax)
{return (val - inMin) * ((outMax - outMin) / (inMax - inMin)) + outMin;
}float MHSensor::readFromUART(HardwareSerial *serial_port)
{long ppmCH4;
byte bufferRead[CH4_DATA_LENGTH];
byte bufferCommand[] = {0xFF, 0x01, 0x86, 0x00, 0x00, 0x00, 0x00, 0x00, 0x79};
serial_port->write(bufferCommand, sizeof(bufferCommand));
serial_port->flush();
int bytesRead = serial_port->readBytes(bufferRead, CH4_DATA_LENGTH);
if (bytesRead != CH4_DATA_LENGTH)
return -1;
```

```
if ((bufferRead[0] == 0xFF) && (bufferRead[1] == 0x86))
{   if (_debug)
{   Serial.println("[INFO] voltage: " + String(getVoltage()));
Serial.println("[INFO] Received bytes: " + (String)bytesRead);

for (int i = 0; i < CH4_DATA_LENGTH; i++)
{   Serial.print(" - Byte");
Serial.print(i);
Serial.print(": ");
Serial.println(bufferRead[i], HEX);
}
long unitIsPpm = ppmCH4 = ((int(bufferRead[2]) * 256) + int(bufferRead[3])) * 100;
Serial.print("[INFO] Byte2 = " + String(bufferRead[2]) + ", Byte3 = " + String(bufferRead[3]));
Serial.print(", Unit is ppm = ");
Serial.println(unitIsPpm);
}
int decimal2 = bufferRead[2];
int decimal3 = bufferRead[3];
ppmCH4 = (decimal2 * 256 + decimal3) * 100;

if (ppmCH4 <= 0)
return 0.0;
return (float)ppmCH4;}
return -1;}
boolean MHSensor::calibrateToZeroPoint(HardwareSerial *serial_port)
{   byte bufferMH440D[CH4_DATA_LENGTH];
byte MH440DCalibrationCommand[] = {0xFF, 0x01, 0x87, 0x00, 0x00, 0x00, 0x00, 0x00, 0x78};
if (_debug)
Serial.println("[INFO] Waiting Calibration MH440D...");
```

```
if (serial_port->availableForWrite() < CH4_DATA_LENGTH)
{
if (_debug)
Serial.println("[WARNING] Failed to Calibration. Retry!");
return false;}
serial_port->write(MH440DCalibrationCommand, sizeof(MH440DCalibrationCommand));
serial_port->flush();
return true;}
////////////////////////////////////////////////////////////////////////////////////////////////////////////////////////////////

// CDM7162 CO2 Sensor Implementation
#include <LiquidCrystal.h>
#include <LcdBarGraph.h>
#include <Wire.h>
#include <stdio.h>

// Pin Definitions
#define INTERRUPT_PIN 2
#define LCD_RS 12
#define LCD_ENABLE 11
#define LCD_D4 6
#define LCD_D5 5
#define LCD_D6 4
#define LCD_D7 3
#define LCD_COLUMNS 16
#define LCD_ROWS 2

// Device and Register Addresses
#define SENSOR_ADDRESS 0x69
```

```
#define REGISTER_ADDRESS 0x03

// LCD and Bar Graph Setup
LiquidCrystal lcd(LCD_RS, LCD_ENABLE, LCD_D4, LCD_D5, LCD_D6, LCD_D7);
LcdBarGraph barGraph(&lcd, LCD_COLUMNS, 0, 1);

// Variables for CO2 Data
byte co2LowerByte = 0;
byte co2UpperByte = 0;
int co2Ppm = 0;
volatile bool sensorStatus = false;
char displayBuffer[8] = {'0', '0', '0', '0', '0', '0', '0', '0'};

void setup() {
  // Pin and Interrupt Setup
  pinMode(INTERRUPT_PIN, INPUT_PULLUP);
  attachInterrupt(digitalPinToInterrupt(INTERRUPT_PIN), onSensorInterrupt, FALLING);

  // Serial and Wire Initialization
  Serial.begin(9600);
  Wire.begin();

  // LCD Initialization
  lcd.begin(LCD_COLUMNS, LCD_ROWS);
  lcd.clear();
  delay(100);
}

void onSensorInterrupt() {
```

```
  sensorStatus = true;
}

void loop() {
  if (sensorStatus) {
    // Read CO2 Data from Sensor
    Wire.beginTransmission(SENSOR_ADDRESS);
    Wire.write(REGISTER_ADDRESS);
    Wire.endTransmission();
    Wire.requestFrom(SENSOR_ADDRESS, 2);

    co2LowerByte = Wire.read();   // Lower Byte
    co2UpperByte = Wire.read();   // Upper Byte
    co2Ppm = (co2UpperByte << 8) | co2LowerByte; // Combine Bytes

    // Print CO2 Level to Serial Monitor
    Serial.println(co2Ppm);

    // Format and Display CO2 Level on LCD
    sprintf(displayBuffer, "%d ppm", co2Ppm);
    lcd.setCursor(0, 0);
    lcd.print(displayBuffer);

    // Update Bar Graph
    barGraph.drawValue(co2Ppm - 400, 1200); // CO2 levels start at 400 ppm

    // Reset Sensor Status
    sensorStatus = false;
    delay(200);
```

```
   }
}
////////////////////////////////////////////////////////////////////////////////////////////////////////////////////////////////////////////////////////
```

ESP 32 OR ARDUINO

```
void setup()
{ pinMode(2, OUTPUT); // put your setup code here, to run once:
}void loop() {
digitalWrite(2,HIGH);// put your main code here, to run repeatedly:
delay(500);
digitalWrite(2,LOW);
delay(1000);}

////////////////////////////////////////////////////////////////////////////////////////////////////////////////////////////////////////////////////////
// Prototype Code for QAPT Project
// Faculty of Sciences, University of Lisbon - 2019
#include <SD.h>
#include <SPI.h>
#include <Wire.h>
#include <math.h>
#include <TimeLib.h>
#include <DS1307RTC.h>
#include <Adafruit_Sensor.h>
#include <Adafruit_BME280.h>
#include <LiquidCrystal_I2C.h>
// Define constants and addresses
#define SEA_LEVEL_PRESSURE_HPA (1013.25)
#define MULTIPLEXER_ADDRESS 0x70
// Sensor and RTC object declarations
Adafruit_BME280 bmeSensor;
```

```
tmElements_t rtcTime;
// SD card configuration
const int sdChipSelect = 4;
// Data logging variables
int logCounter = 1;
File logFile;

// LCD setup with I2C address
LiquidCrystal_I2C lcd(0x27, 2, 1, 0, 4, 5, 6, 7, 3, POSITIVE);
// RGB LED pin assignments
const int redPin = 2;    // Red LED pin
const int bluePin = 3;   // Blue LED pin
const int greenPin = 7;  // Green LED pin
// NH3 sensor data handling
int sensorIndex = 0;
int nh3Readings[3];
int humidityReadings[3];
int tempReadings[3];
int altitudeReadings[3];
int avgNH3 = 0;
int avgHumidity = 0;
int avgTemperature = 0;
int avgAltitude = 0;
int calibratedNH3PPM = 0;
int nh3Sum = 0;
int humiditySum = 0;
int tempSum = 0;
int altitudeSum = 0;
////////////////////////////////////////////////////////////
```

```
// TCA9548A I2C multiplexer function:
void tcaselect(uint8_t i) {
if (i > 7) return;
Wire.beginTransmission(TCAADDR);
Wire.write(1 << i);
Wire.endTransmission();
}
////////////////////////////////////////////////////////////////////////
void setup() {
Serial.begin(9600);
lcd.begin(16, 2);
pinMode(redpin, OUTPUT);
pinMode(bluepin, OUTPUT);
pinMode(greenpin, OUTPUT);
Serial.print("Initializing SD card...");
// see if the card is present and can be initialized:
if (!SD.begin(chipSelect)) {
Serial.println("Card failed, or not present");
// don't do anything else:
while (1);
}
Serial.println("card initialized.");
File dataFile = SD.open("datalog1.csv", FILE_WRITE);
if (dataFile) {
dataFile.println(" , , , , , ,"); //line to separate datasets
String Header = "Date, Time, RH[%], T[oC], Height[m], [NH3]";
dataFile.println(Header);
dataFile.close();
Serial.println(Header);
```

```
} else {
Serial.println("Couldn't open log file");
}
//initialize the BME280 sensor:
tcaselect(4);
if (!bme1.begin(0x76)) {
/* There was a problem detecting the bme1 ... check your connections */
Serial.println("Ooops, no bme1 detected ... Check your wiring!");
}
//Heating time...
Serial.println("Please wait...Preparing system.");
//write to LCD:
tcaselect(2);
///set the cursor to (0,0):
lcd.setCursor(0,0);
lcd.print("Please wait...");
72
Development of an ammonia portable low-cost air quality station
/// set the cursor to (16,1):
lcd.setCursor(0,1);
lcd.print("Preparing system");
delay(900000); //Heating time of the MQ137 resistance
Serial.println("Ready!!!");
lcd.setCursor(0,0);
lcd.print("Ready!!!
");
lcd.setCursor(0,1);
lcd.print("
}
```

```
");
//////////////////////////////////////////////////////////
void loop() {
const int MQ137_PIN = A3;
const float RL_MQ137 = 1.0;
// kohm (FC-22 module = 1.0 kohm)
const float CLEAN_AIR_RATIO_MQ137 = 3.6;
float sensorValue_MQ137;
float sensor_volt_MQ137;
float Rs_MQ137;
// kohm
// Taken from datasheet graph
const float R0_MQ137 = 16.10;  // kohm , from the R0 finder sketch
float AirFraction_MQ137;
float AirFractionMin_MQ137 = 0.118851;
float AirFractionMax_MQ137 = 0.388153;
float AirFractionCurva33_MQ137;
float AirFractionCurva85_MQ137;
float AirFractionCalibr_MQ137;
//Calculating Rs from analog data
sensorValue_MQ137 = analogRead(A3);
sensor_volt_MQ137 = sensorValue_MQ137*(5.0/1023.0); //Convert to voltage
Rs_MQ137 = ((5.0*RL_MQ137)/sensor_volt_MQ137)-RL_MQ137; //Calculate Rs
AirFraction_MQ137 = Rs_MQ137/R0_MQ137;
//Get RTC date and time:
tcaselect(7);
RTC.read(tm);
int Day = tm.Day;
int Month = tm.Month;
```

```
int Year = tmYearToCalendar(tm.Year);
int Hour = tm.Hour;
int Minute = tm.Minute;
int Second = tm.Second;
//Get BME280 sensor data
tcaselect(4);
float h1 = bme1.readHumidity()+6.89;
int h1round = h1;
float t1 = bme1.readTemperature()+0.55;
int t1round = t1;
float Alt1 = bme1.readAltitude(1013.25)+45;
int Alt1round = Alt1;
```



```
float ppmNH3calibr;
float ppmNH3;
//  Calibration of MQ137 considering Temperature and relative humidity based
on Hanwen datasheet, using polinomial regression
AirFractionCurva33_MQ137 = 0.0003 * pow(t1, 2) - 0.0255 * t1 + 1.4004;
AirFractionCurva85_MQ137 = 0.0003 * pow(t1, 2) - 0.0231 * t1 + 1.2808;
if (h1 >= 0 && h1 < 59) {
AirFractionCalibr_MQ137 = AirFraction_MQ137 / AirFractionCurva33_MQ137;
}
else {
AirFractionCalibr_MQ137 = AirFraction_MQ137 / AirFractionCurva85_MQ137;
}
/// Convertion to ppm of NH3:
float expoente_MQ137 = 1 / (-0.257);
ppmNH3 = pow((AirFraction_MQ137 / 0.587), expoente_MQ137);
```

```
ppmNH3calibr = pow((AirFractionCalibr_MQ137 / 0.587), expoente_MQ137);
//round [NH3] to an int and then put the values of [NH3], RH and T in the
respective arrays:
for (i=0; i<=2;i=i+1){
ppmNH3calibrround=round(ppmNH3calibr);
mySensValsNH3[i]=ppmNH3calibrround;
sumNH3=sumNH3+mySensValsNH3[i];
mySensValsh1[i]=h1round;
sumh1=sumh1+mySensValsh1[i];
mySensValst1[i]=t1round;
sumt1=sumt1+mySensValst1[i];
mySensValsAlt1[i]=Alt1round;
sumAlt1=sumAlt1+mySensValsAlt1[i];
if(i==2){
//mean of the 3 last values measured
NH3mean=sumNH3/3;
h1mean=sumh1/3;
t1mean=sumt1/3;
Alt1mean=sumAlt1/3;
tcaselect(2);
lcd.setCursor(0,0);
lcd.print("T:");
lcd.print(t1mean);
lcd.print("oC
");
lcd.print("RH:");
lcd.print(h1mean);
lcd.print("% ");
lcd.setCursor(0,1);
```

```
lcd.print("NH3:");
lcd.print(NH3mean);
lcd.print("ppm
}
");
// Change the colour of the RGB LED according to [NH3]
if (NH3mean >= 5 && NH3mean <= 200) {
if (NH3mean <= 25) {
74
Development of an ammonia portable low-cost air quality station
analogWrite(greenpin, 150);
analogWrite(bluepin, 0);
analogWrite(redpin, 0);
} else {
if (NH3mean <= 80) {
analogWrite(bluepin, 150);
analogWrite(greenpin, 0);
analogWrite(redpin, 0);
} else {
analogWrite(redpin, 150);
analogWrite(greenpin, 0);
analogWrite(bluepin, 0);
}
}
} else {
if (NH3mean < 5) {
lcd.setCursor(0,1);
lcd.print("[NH3] OutOfRange");
analogWrite(greenpin, 150);
```

```
analogWrite(redpin, 0);
analogWrite(bluepin, 0);
} else {
lcd.setCursor(0,1);
lcd.print("[NH3] OutOfRange");
analogWrite(redpin, 150);
analogWrite(greenpin, 0);
analogWrite(bluepin, 0);
}
}
delay(1000);
}
//create strings
String dataString1 = String(Day) + "/" + String(Month) + "/" + String(Year)
+ "," + String(Hour) + ":" + String(Minute) + ":" + String(Second) + ",";
String dataString2 = String(h1mean) + "," + String(t1mean) + "," +
String(Alt1mean) + "," + String(NH3mean);
// open file (only one at a time)so you have to close this one before opening
another
File dataFile1 = SD.open("datalog1.csv", FILE_WRITE);
// if the file is available, write to it:
if (dataFile1) {
dataFile1.print(dataString1);
dataFile1.println(dataString2);
dataFile1.close();
}
// if the file isn't open, pop up an error:
else {
Serial.println("error opening datalog1.csv");
```

```
}
Serial.print(dataString1);
Serial.print(dataString2);
75
Development of an ammonia portable low-cost air quality station
Serial.println();
Serial.println();
Serial.println();
//reset the values for the next loop
i=-1;
sumNH3=0;
sumh1=0;
sumt1=0;
sumAlt1=0;
}
////////////////////////////////////////////////////////////////////////////////////////////////////////////////////////////////
```

1. ***Check Threshold***:

Implementation Code (Arduino-compatible)

```
#include <Wire.h>
#include "SHT3x.h" // Library for SHT35 sensor
// Configuration constants
const float HEAT_INDEX_LIMIT = 72.0; // Heat stress threshold
const int SENSOR_READ_DELAY = 5000;  // Interval between sensor readings (ms)
// Sensor instance
SHT3x temperatureHumiditySensor(SDA, SCL);
void setup() {
  Serial.begin(9600);
```

```
  if (!temperatureHumiditySensor.begin()) {
    Serial.println("Error: Unable to initialize SHT35 sensor!");
    while (1); // Halt execution
  }
  Serial.println("Environmental Monitoring System Ready");
}
void loop() {
  float currentTemperature, currentHumidity;
  // Fetch data from the SHT35 sensor
  if (temperatureHumiditySensor.get() == 0) {
    currentTemperature = temperatureHumiditySensor.cTemp; // Temperature in Celsius
    currentHumidity = temperatureHumiditySensor.humidity; // Relative Humidity in percentage
  } else {
    Serial.println("Error: Sensor data retrieval failed!");
    delay(SENSOR_READ_DELAY);
    return;
  }
  // Convert Relative Humidity (RH) to a decimal fraction
  float rhDecimal = currentHumidity / 100.0;
  // Compute Temperature-Humidity Index (THI)
  float heatIndex = currentTemperature + (0.36 * currentTemperature * rhDecimal) + 41.2;
  // Assess THI value against the defined threshold
  if (heatIndex > HEAT_INDEX_LIMIT) {
    Serial.print("Warning: THI threshold exceeded! Current Value: ");
```

```
        Serial.println(heatIndex);
    } else {
        Serial.print("THI is within the acceptable range: ");
        Serial.println(heatIndex);
    }
    // Pause before the next cycle
    delay(SENSOR_READ_DELAY);
}
////////////////////////////////////////////////////////////////////////////////////////////////////////////////////////////////////////
# Constants: Safe threshold values for gases (in ppm)
THRESHOLDS = {
    "ammonia": 25,        # Safe limit for NH₃
    "carbon_dioxide": 2000,  # Safe limit for CO₂
    "methane": 100,       # Safe limit for CH₄
}
# Monitoring intervals (e.g., data recorded every 10 minutes)
TIME_INTERVAL_MINUTES = 10
# Variables to store daily stress load values (DSLV) and stress duration (DSD) for each gas
stress_load = {
    "ammonia": 0,
    "carbon_dioxide": 0,
    "methane": 0,
}
stress_duration = {
```

```
    "ammonia": 0,
    "carbon_dioxide": 0,
    "methane": 0,
}
# Function to evaluate stress load and duration
def evaluate_stress(gas_concentrations):
    """
    Evaluate stress load and duration based on current gas concentrations.
    Args:
        gas_concentrations (dict): Current gas concentrations in ppm (e.g., {"ammonia": 30, "carbon_dioxide": 2500, "methane": 150})
    """
    global stress_load, stress_duration
    for gas, concentration in gas_concentrations.items():
        if concentration > THRESHOLDS[gas]:
            # Add to stress load (amount exceeding the threshold)
            stress_load[gas] += concentration - THRESHOLDS[gas]

            # Increment stress duration
            stress_duration[gas] += TIME_INTERVAL_MINUTES


# Function to reset daily values for a new day
def reset_daily_values():
    """
```

```
    Reset daily stress load and stress duration for the next day.
    """
    global stress_load, stress_duration

    stress_load = {key: 0 for key in stress_load}
    stress_duration = {key: 0 for key in stress_duration}

# Example simulation
if __name__ == "__main__":
    import time
    import random

    # Simulating a day's worth of data (e.g., 144 intervals for a 10-minute interval in 24 hours)
    for interval in range(144):  # 24 hours * 60 minutes / 10 minutes = 144
        # Simulated gas concentrations (ppm)
        current_gas_concentrations = {
            "ammonia": random.randint(10, 40),        # Random NH₃ value between 10 and 40
            "carbon_dioxide": random.randint(1500, 2500),   # Random CO₂ value between 1500 and 2500
            "methane": random.randint(50, 150),       # Random CH₄ value between 50 and 150
        }
        # Evaluate stress for the current interval
        evaluate_stress(current_gas_concentrations)
```

```
    # Simulate real-time interval (optional, for demonstration)
    time.sleep(0.01)  # Fast-forward simulation (use time.sleep(600) for real 10-minute intervals)

# Print daily results
print("Daily Stress Load Values (DSLV):", stress_load)
print("Daily Stress Durations (DSD, in minutes):", stress_duration)

# Reset values for the next day
reset_daily_values()
```